A few projects with Quantum ESPRESSO
a personal selection

Stefano de Gironcoli

SISSA and CNR-IOM DEMOCRITOS

Controlling morphology of Au_{20} clusters by substrate doping

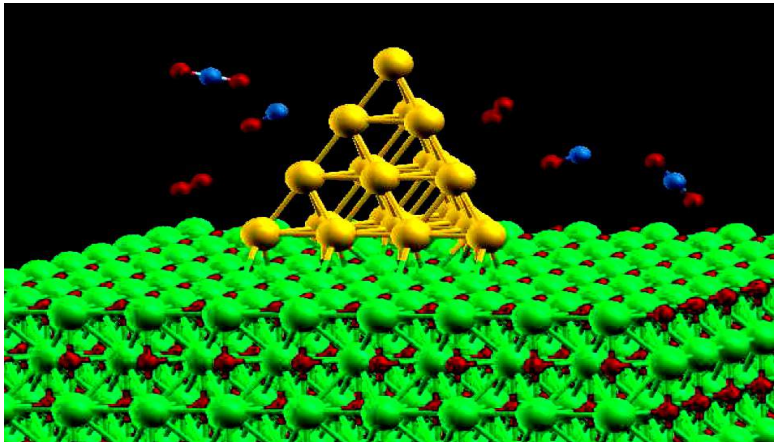

^{27}Al NMR shifts of Alumina and its precursors

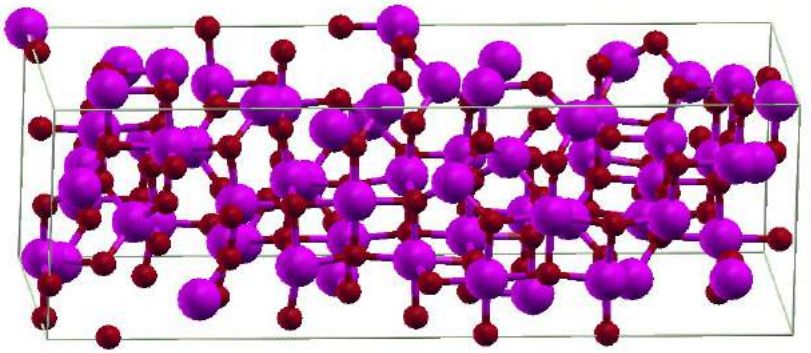

ζ-Glycine: Insight into the mechanism of a polymorphic phase transition

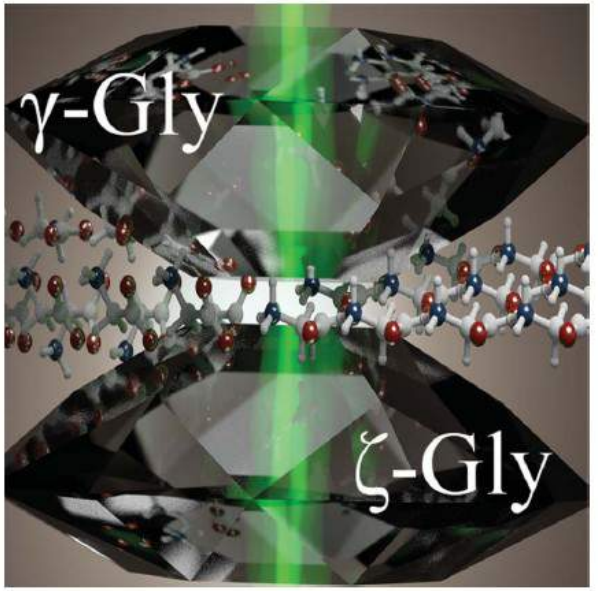

Complete ^{13}C Chemical Shift Assignment for Cholesterol Crystal

Controlling morphology of Au_{20}^- clusters by substrate doping

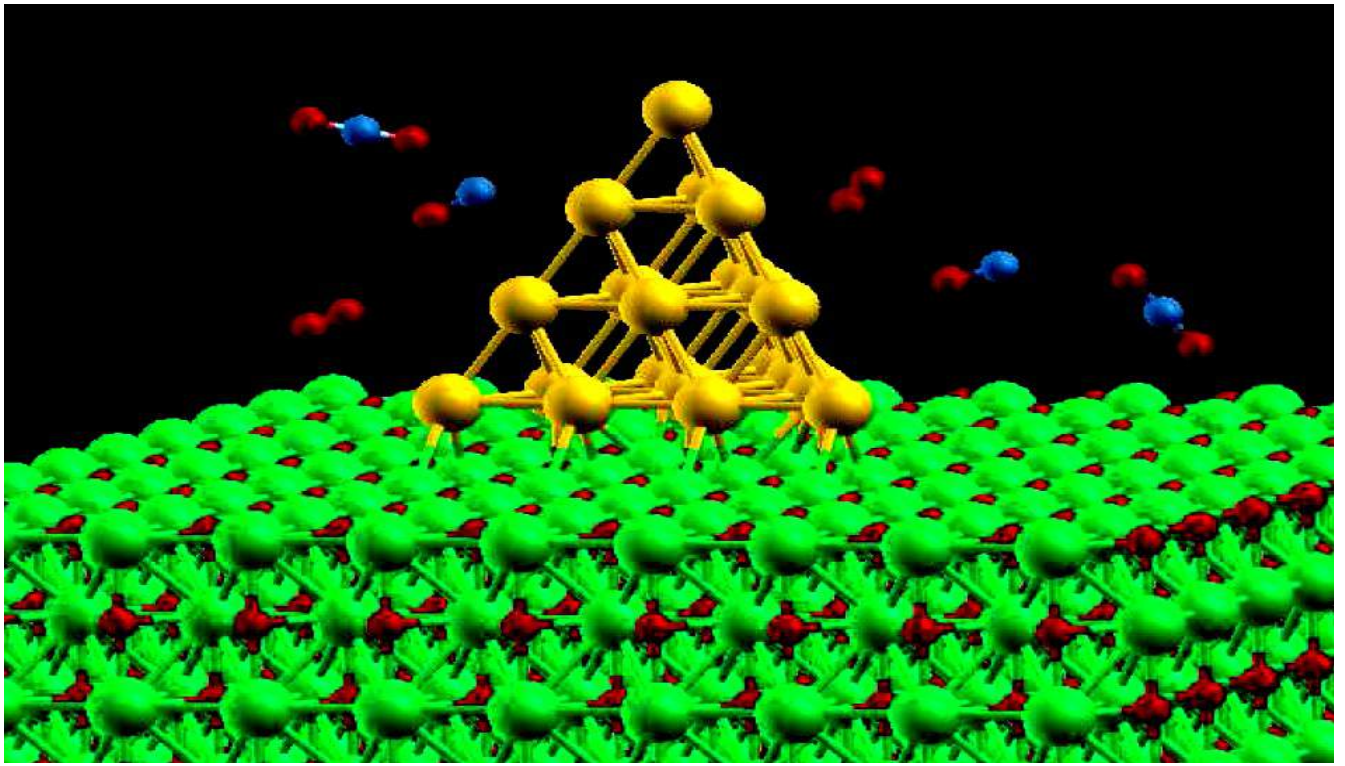

Catalytic Activity of Gold

- Bulk gold → inert;
- nanoclusters → good catalysts
- Most important reaction: CO oxidation to CO_2
  - In automobile exhaust
  - Prevent CO poisoning in fuel cells

Vehicle exhaust emissions

http://saferenvironment.wordpress.com

- negatively charged cluster showed excellent CO conversion yields and rates[1]

- conversion rate dependent on size and shape of cluster

- Au_{20} - extremely robust[2] to distortions when supported over an MgO surface, keeping its tetrahedral structure

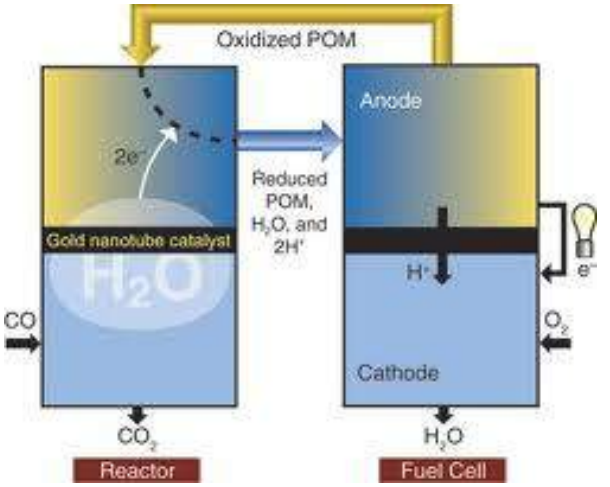

http://comdig.unam.mx/index.php?id_issue=2004.35

1. B. Yoon, et al . Science 307 (2005) 403
2. J. Li, Xi Li, H. Zhai, L. Wang, Science 299 (2003)

Problem and Motivation

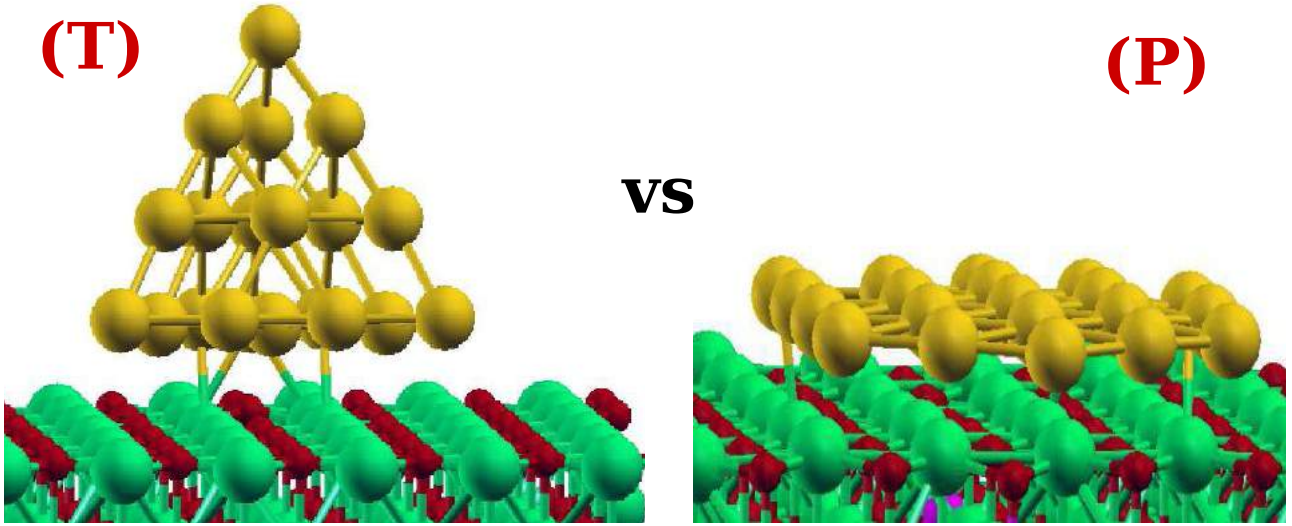

Why Au(P) desirable over Au(T)?

(1) more charge absorbed from substrate
(2) more surface area
(3) more sites of high charge accumulation → more active sites for reaction
(4) better catalytic activity for oxidation reactions

Possible Methods

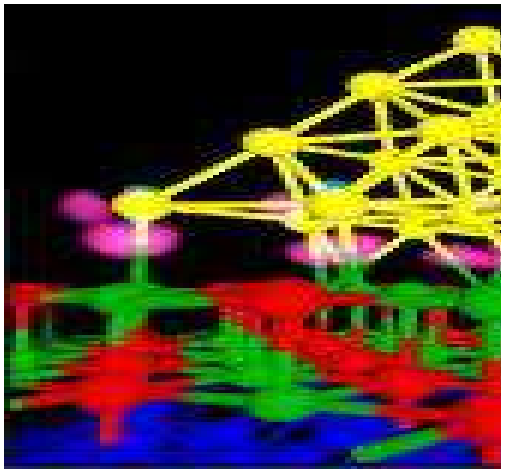

How to favor (P) over (T) ?

- MgO support? — No
- F-center defect rich MgO?[1] — No
- Thin oxide layer over metal support?[2] — **Yes!**
- Placing system in high electric field?[3] — **Yes!**

} Impractical for applications

Look for better solution …

1. Z. Yan, D. W. Goodman, JACS 127 (2005), 1604.
2. C. Harding, U. Landman, J. Am. Chem. Soc. 131 (2009) 538.
3. B. Yoon, U Landman, PRL 100 (2008) 056102.

Technical Details

- Quantum ESPRESSO package used
- Plane wave energy cut-off 30 Ry, charge density cut-off 240 Ry
- Exchange-correlation functional – GGA
- Ultrasoft pseudopotentials used, scalar relativistic pseudopotentials used for Au
- Smearing – Marzari-Vanderbilt
- Bulk calculations on MgO and Al-doped MgO – $3 \times 3 \times 3$ cells used
- Slab calculations on MgO, Al-doped MgO, substrate supported Au clusters – 6×6 cell with 4 layers of substrate and 14 Å vacuum considered
- k-point sampling at gamma point

Our proposed solution

- Mg [Ne] $3s^2$
- Al [Ne] $3s^2$, $3p^1$

- Doping of MgO with Al → extra electron of Al delocalized in MgO → charge transfer to Au cluster → **(P) favored ??**

Density of States

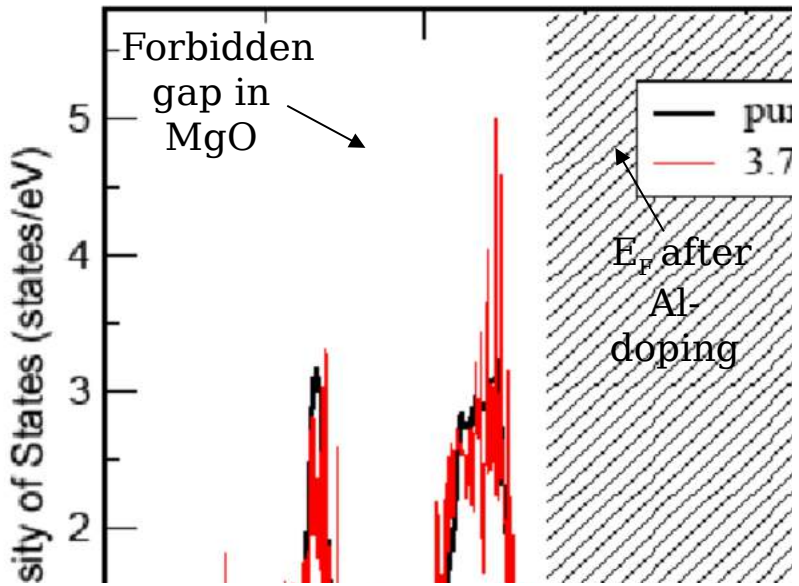

- Shift of the Fermi level into the conduction band on doping

Work Function

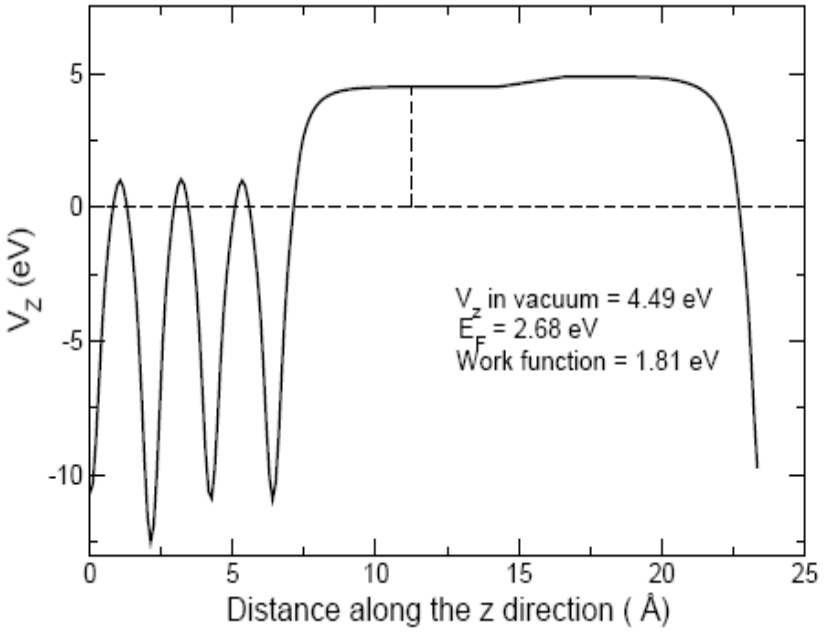

- Work function on doping (conc. 2.78%) = 1.81 eV.

Results on Au_{20} free clusters

(T)

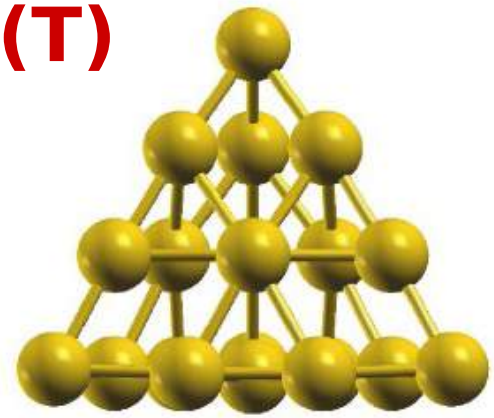

(a)

Binding energy
=1.14 eV/atom

Shortest NN bond
dist = 2.69 Å

(P)

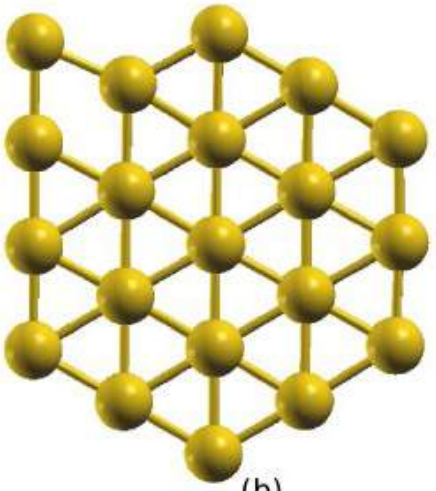

(b)

Binding energy
=1.06 eV/atom

Shortest NN bond
dist = 2.70 Å

Tetrahedral (T) structure favored over planar (P) structure in vacuum by 1.52 eV

(in agreement with earlier results)

Main Result

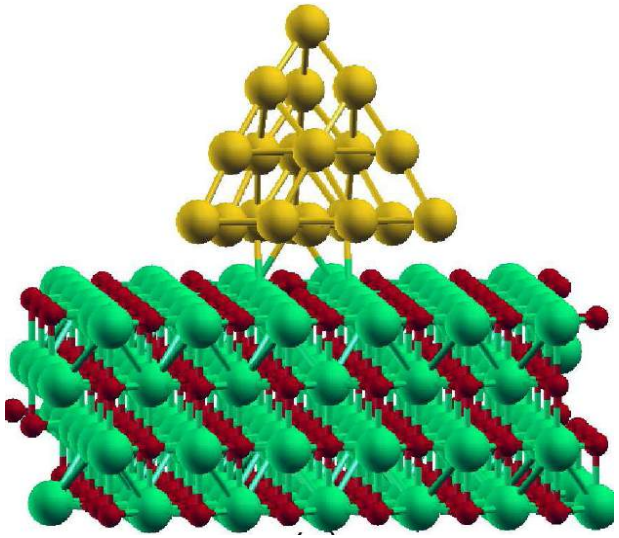

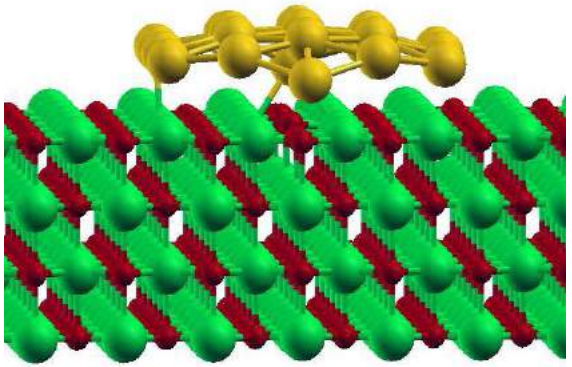

Au_{20} on pure MgO

Au(T) favored over Au(P) by 0.60 eV

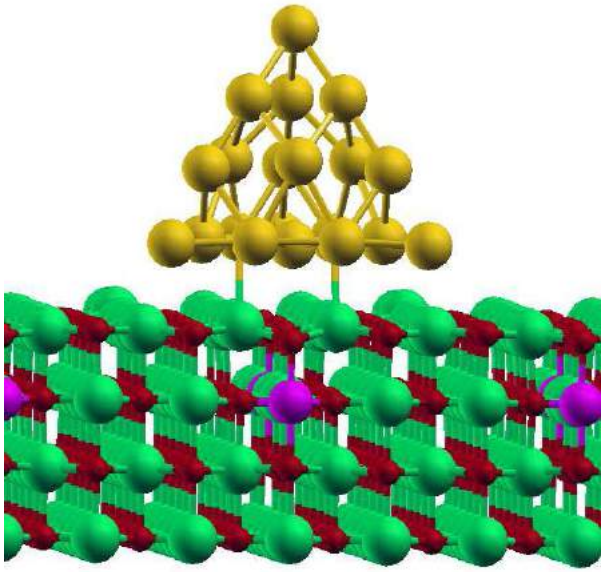

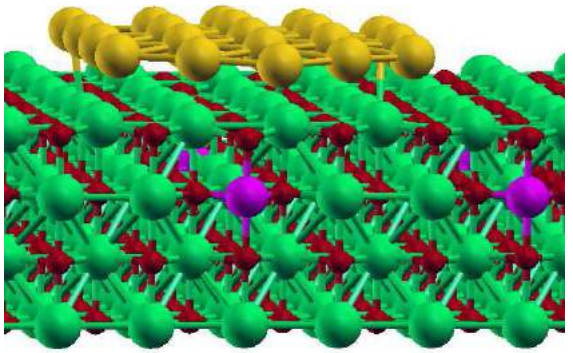

Au_{20} on Al-doped MgO

Various conc.s studied

Au(P) favored over Au(T) by value dependent on conc.

Au clusters on Al-doped MgO

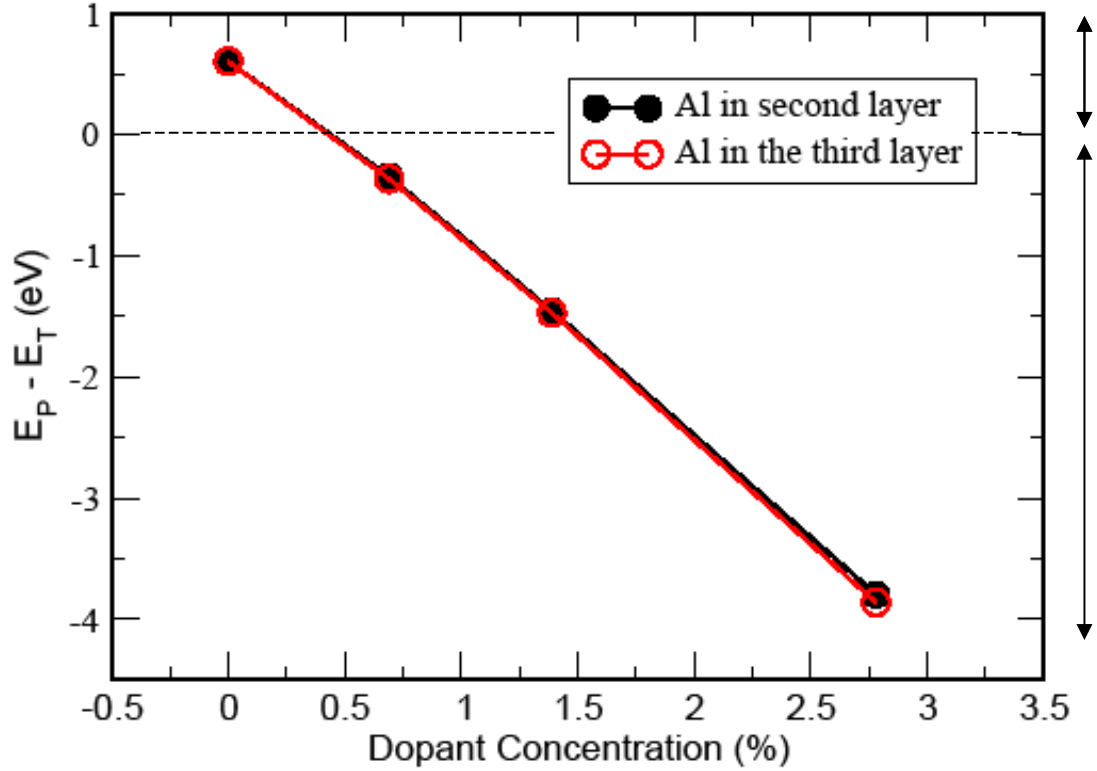

(T) favored

(P) favored

- ~ Linear relationship between dopant concentration and stability of (P) structure over (T) obtained.
- Results not very sensitive to position of Al atoms
- Minimum conc. of Al required to flip geometry of Au cluster = 0.4 %

Charge transfer from substrate to cluster

Au(P)

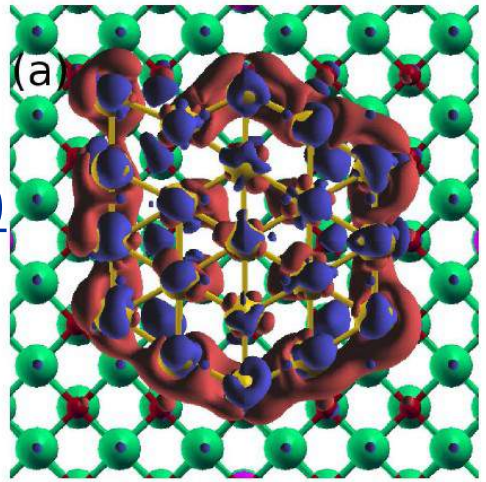

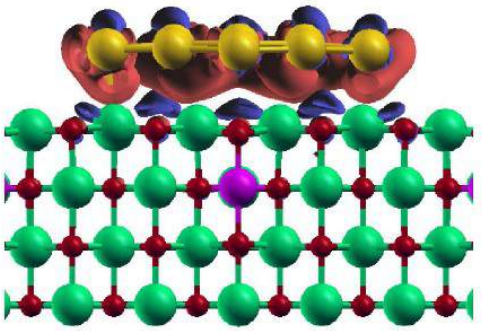

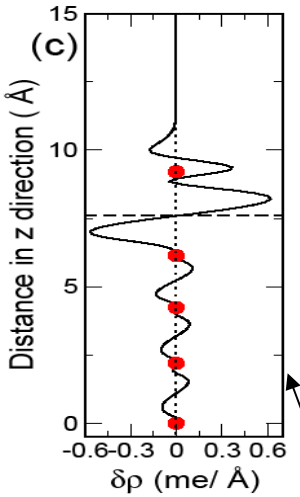

Charge Transfer = 1.12 e

0.0025 e/Å³ isosurface plots

Planar average of charge transfer

Au(T)

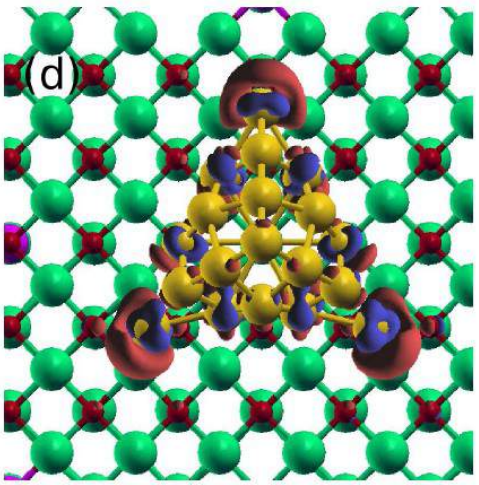

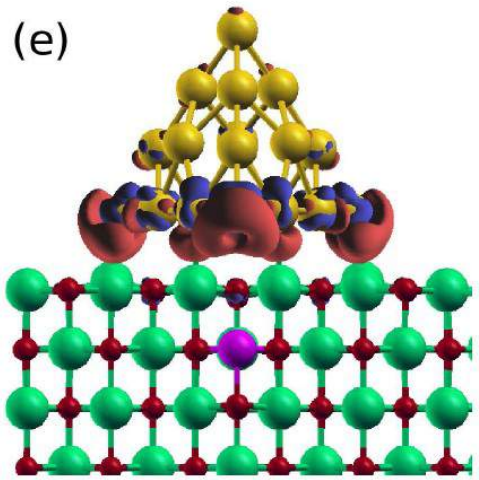

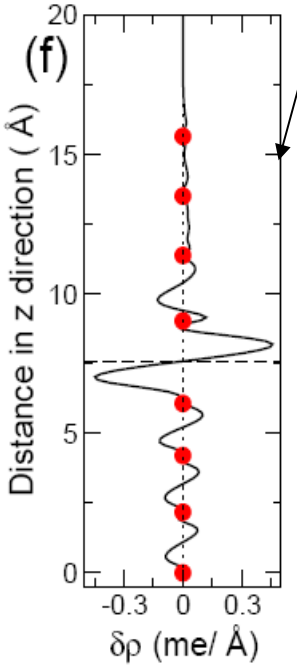

Charge Transfer = 0.89 e

0.0013 e/Å³ isosurface plots

Conclusions

- Doping of MgO results in dimensionality crossover of Au_{20} cluster from (T) to (P)
- Linear relation between dopant concentration and energy difference between (P) and (T) observed.
- Why our method?

  (1) preparation of metal-supported MgO difficult

  (2) electric field applied (1 V/nm) too high

  (3) Al dopant atoms may act as anchor sites for Au clusters

Credits

Nisha Mariam Mammen

Shobhana Narasimhan

TSU-JNCASR, Bangalore

NMR properties of Materials from Density Functional Perturbation Theory

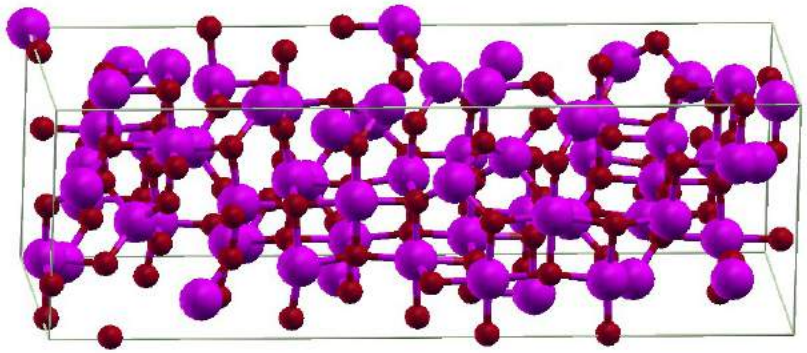

Outline

- Theory (GIPAW +PAW)

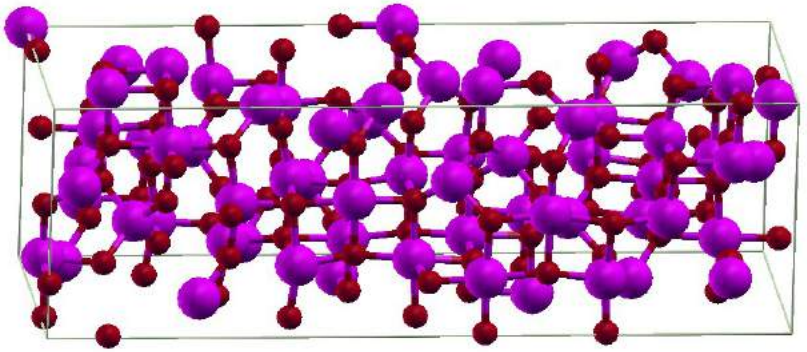

- ^{27}Al NMR shifts of alumina and its precursors

- ^{13}C NMR of Cholesterol Crystals

Outline

- Theory (GIPAW +PAW)

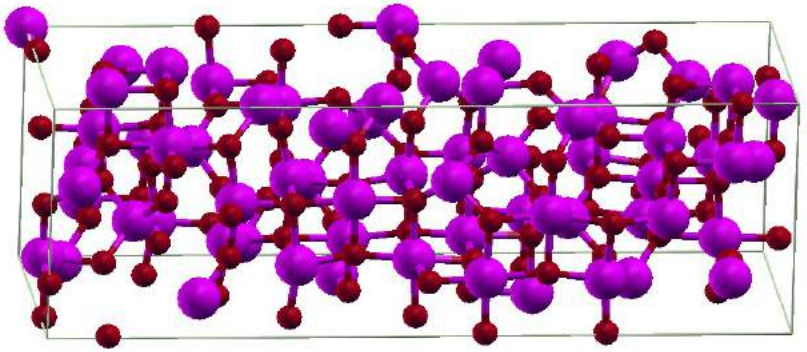

- ^{27}Al NMR shifts of alumina and its precursors

- ^{13}C NMR of Cholesterol Crystals

Theory : NMR Chemical Shifts

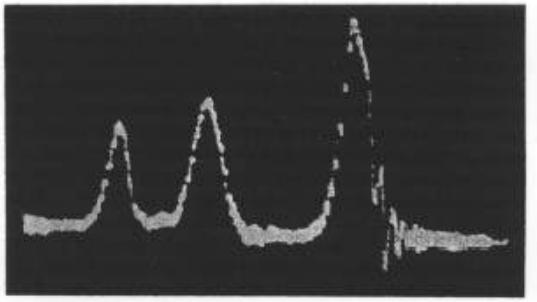

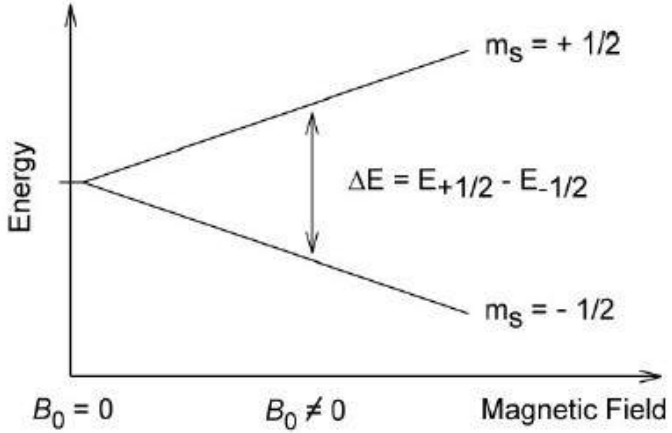

$$\Delta E = \hbar \gamma B_{\text{tot}} \Delta m_s = \hbar\omega$$
$$B_{\text{tot}} = B_{\text{ext}} + B_{\text{ind}} + B_{\text{other}}$$

Arnold, Dhamatti Packard, JCP **19,** 507 (1951)

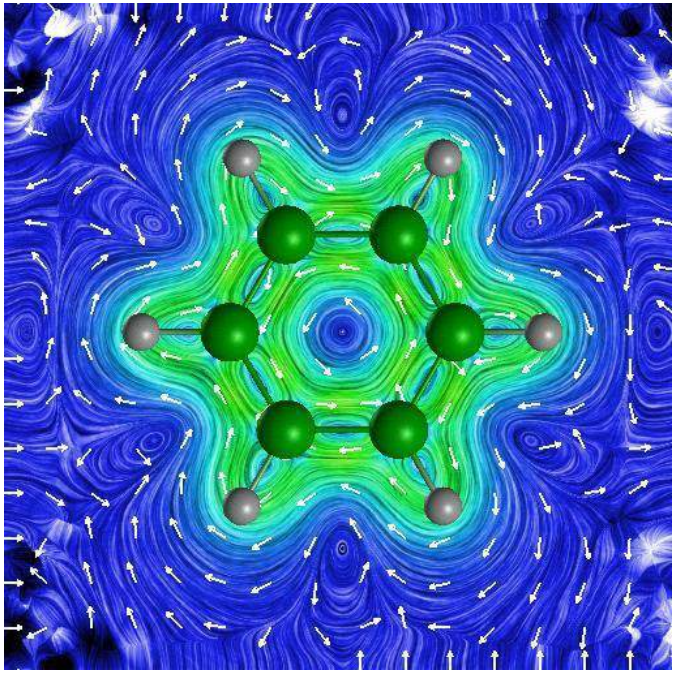

Theory : NMR Chemical Shifts

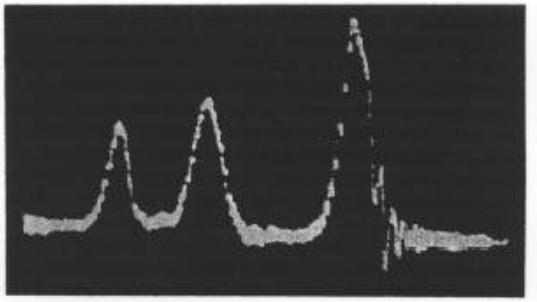

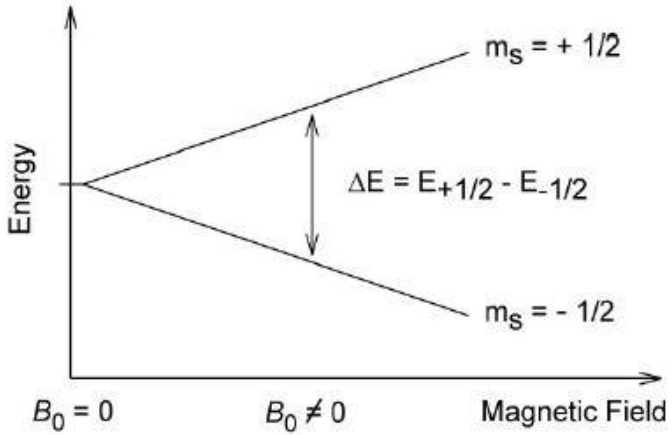

$$\Delta E = \hbar \gamma B_{\text{tot}} \Delta m_s = \hbar \omega$$
$$B_{\text{tot}} = B_{\text{ext}} + B_{\text{ind}} + B_{\text{other}}$$

Arnold, Dhamatti Packard, JCP **19,** 507 (1951)

shielding tensor

$$\mathbf{B}_{\text{eff}} = \mathbf{B}_{\text{ext}}\left(1 - \overleftrightarrow{\sigma}\right)$$

- independent of magnetic field
- usually << 1
- measured in ppm (1 ppm = 10^-6)

chemical shift

$$\delta = -\left(\sigma - \sigma_{\text{ref}}\right)$$

- given as deviation from a reference
- TMS(1H,13C,29Si)
- measured in ppm (1 ppm = 10^-6)

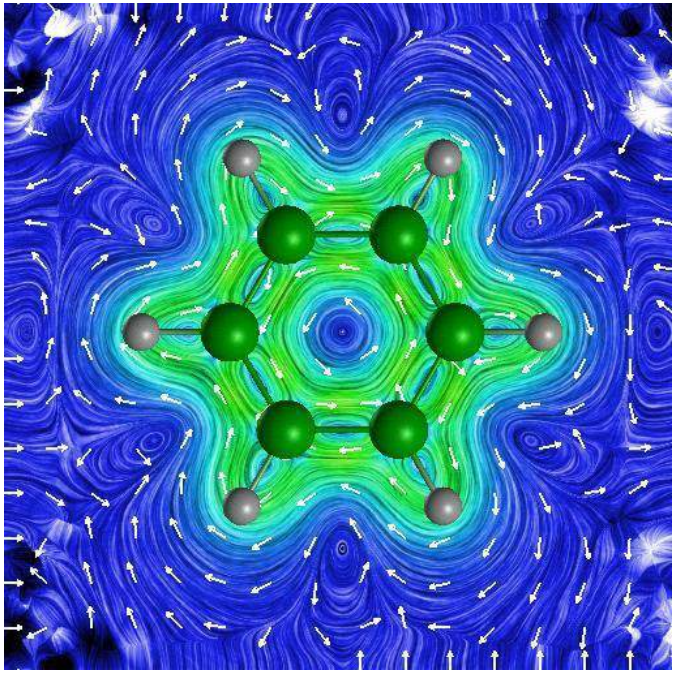

Theory : NMR Chemical Shifts

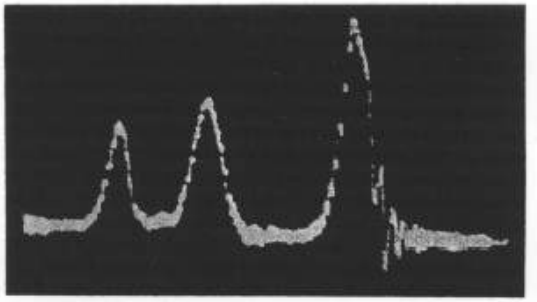

Arnold, Dhamatti Packard, JCP **19,** 507 (1951)

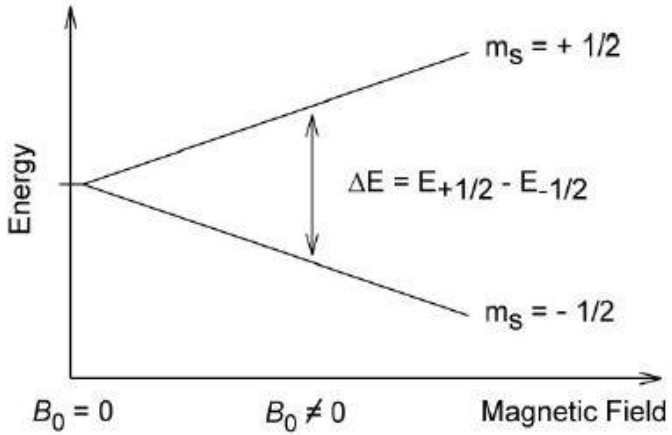

$$\Delta E = \hbar \gamma B_{\text{tot}} \Delta m_s = \hbar\omega$$
$$B_{\text{tot}} = B_{\text{ext}} + B_{\text{ind}} + B_{\text{other}}$$

shielding tensor $\mathbf{B}_{\text{eff}} = \mathbf{B}_{\text{ext}}(1 - \overleftrightarrow{\sigma})$

- independent of magnetic field
- usually << 1
- measured in ppm (1 ppm = 10^-6)

chemical shift $\delta = -(\sigma - \sigma_{\text{ref}})$

- given as deviation from a reference
- TMS(1H,13C,29Si)
- measured in ppm (1 ppm = 10^-6)

Other NMR interactions

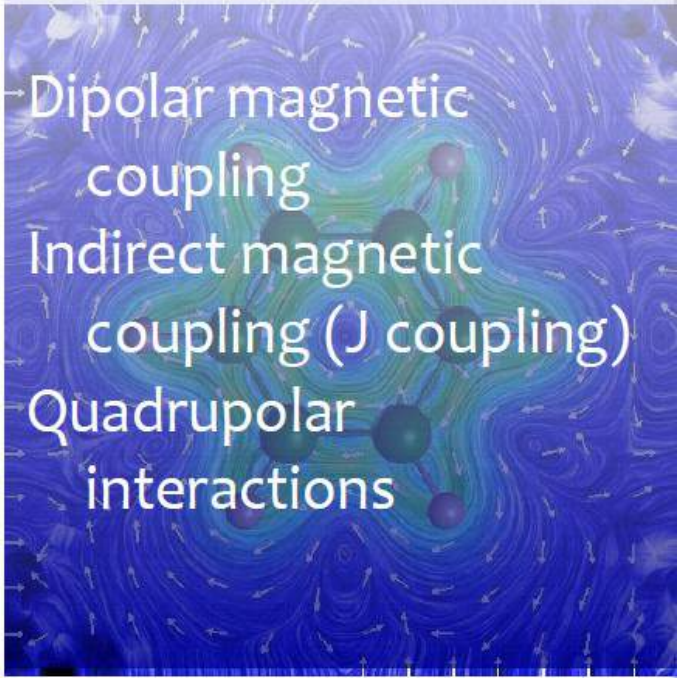

PHYSICAL REVIEW B, VOLUME 63, 245101

All-electron magnetic response with pseudopotentials: NMR chemical shifts

Chris J. Pickard*
Institut für Geowissenschaften, Universität Kiel, Olshausenstrasse 40 D-24098 Kiel, Germany

Francesco Mauri
Laboratoire de Minéralogie-Cristallographie de Paris, Université Pierre et Marie Curie, 4 Place Jussieu, 75252, Paris, Cedex 05, France
(Received 17 November 2000; published 10 May 2001)

- Density Functional Perturbation Theory :

$$\left|\phi_n^{(0)}\right\rangle \longrightarrow \left|\phi_n^{(1)}\right\rangle \longrightarrow \mathbf{j}_{\mathrm{ind}}(\mathbf{r}) \longrightarrow \mathbf{B}_{\mathrm{ind}}(\mathbf{r})$$

$$\mathbf{B}_{\mathrm{ind}}(\mathbf{r}) = \frac{1}{c}\int d^3\mathbf{r}' \, \frac{\mathbf{j}_{\mathrm{ind}}(\mathbf{r}') \times (\mathbf{r}-\mathbf{r}')}{|\mathbf{r}-\mathbf{r}'|^3}$$

$$\mathbf{B}_{\mathrm{ind}} = -\bar{\bar{\sigma}}\mathbf{B}_{\mathrm{ext}}$$

Gauge-Including Projector-Augmented Wave

Blochl, PRB50, 17953 (1994)

$$|\Psi\rangle = \mathcal{T}|\tilde{\Psi}\rangle$$

valence wfcs

$$|\psi^{\mathrm{AE}}\rangle = |\psi^{\mathrm{PS}}\rangle + \sum_{R,n} \left(|\phi^{\mathrm{AE}}_{r,n}\rangle - |\phi^{\mathrm{PS}}_{R,n}\rangle\right) \langle p_{R,n}|\psi^{\mathrm{PS}}\rangle$$

atomic partial waves

atomic projectors

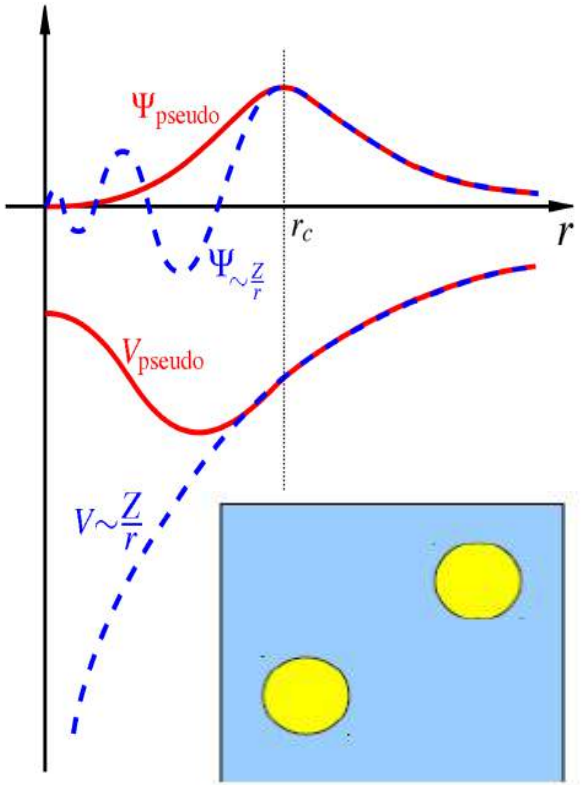

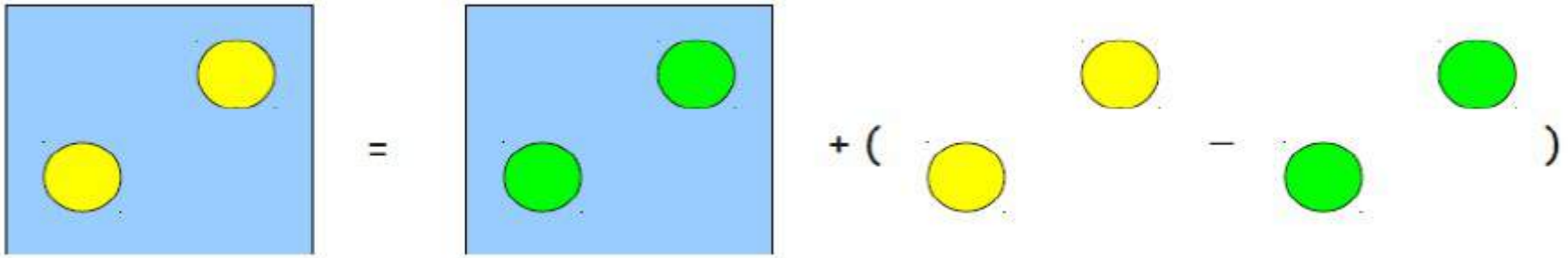

gauge origin problem

Under uniform magnetic field B , one center

$$H=\frac{1}{2}\left(\mathbf{p}+\frac{1}{c}\mathbf{A}(\mathbf{r})\right)^2+V(\mathbf{r}) \qquad \mathbf{A}(\mathbf{r})=\frac{1}{2}\mathbf{B}\times(\mathbf{r}-\mathbf{d})$$

$$H=\frac{1}{2}\mathbf{p}^2+V(\mathbf{r})+\frac{1}{2c}\mathbf{L}\cdot\mathbf{B}+\frac{1}{8c^2}(\mathbf{B}\times\mathbf{r})^2$$

$$\tilde{O}=O+\sum_{ij}|\tilde{p}_i\rangle[\langle\phi_i|O|\phi_j\rangle-\langle\tilde{\phi}_i|O|\tilde{\phi}_j\rangle]\langle\tilde{p}_j|$$

More than one center

$$H'=\frac{1}{2}\left(\mathbf{p}+\frac{1}{c}\mathbf{A}(\mathbf{r})\right)^2+V(\mathbf{r}-\mathbf{t}) \qquad \Psi'(\mathbf{r})=e^{(i/2c)\mathbf{r}\cdot\mathbf{t}\times\mathbf{B}}\Psi(\mathbf{r})$$

Gauge Including PAW

$$\mathcal{T}=1+\sum_{\mathbf{R},n}(|\phi_{\mathbf{R},n}\rangle-|\tilde{\phi}_{\mathbf{R},n}\rangle)\langle\tilde{p}_n|$$

$$\mathcal{T}_{\mathbf{B}}=1+\sum_{\mathbf{R},n}e^{(i/2c)\mathbf{r}\cdot\mathbf{R}\times\mathbf{B}}[|\phi_{\mathbf{R},n}\rangle-|\tilde{\phi}_{\mathbf{R},n}\rangle]\langle\tilde{p}_{\mathbf{R},n}|e^{-(i/2c)\mathbf{r}\cdot\mathbf{R}\times\mathbf{B}}$$

GIPAW developments

Originally implemented by Pickard and Mauri [Phys. Rev. B 63, 245101 (2001)] for Norm-Conserving PseudoPotentials only.

Extended to UltraSoft PseudoPotentials by Yates, Pickard and Mauri [Phys. Rev. B 76, 024401 (2007)]

Ported to Quantum ESPRESSO and extended to PAW by Emine Kucukbenli.

All-electron quality calculations are now possible, no extra generation needed w.r.t. PAW datasets used in the scf cycle

Outline

- Theory (GIPAW +PAW)

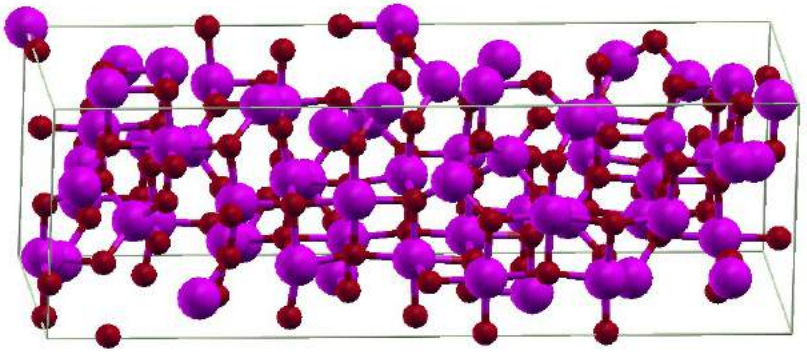

- ^{27}Al NMR shifts of alumina and its precursors

- ^{13}C NMR of Cholesterol Crystals

Alumina and its calcination precursors

Aluminium oxide (Al_2O_3), also known as alumina, is one of the most important oxides because of its many industrial applications.

Corundum (α-Al_2O_3),the most stable crystalline form of alumina, is the final product of the calcination of hydroxides or oxyhydroxides of aluminium at elevated temperature.

The transformation from aluminium hydrates to the final oxide involves a variety of relatively stable transitional intermediate phases.

γ-Al_2O_3 is particularly valued for its applications as catalyst and catalyst support in petrochemical applications.

Its crystal structure is still poorly known

Alumina and its calcination precursors

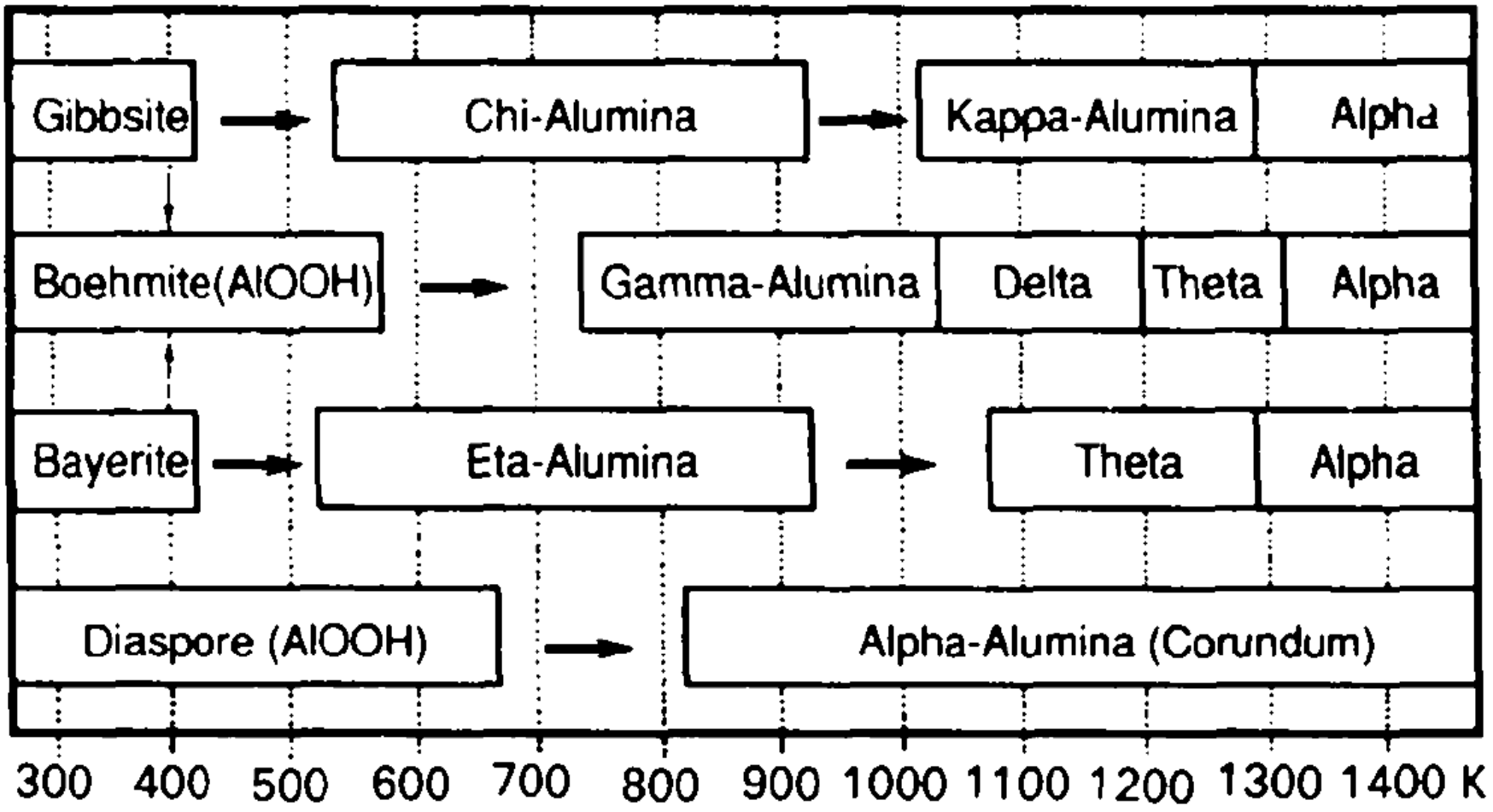

Thermal diagram of transition alumina (after Wefers & Misra, 1987)

NMR Spectra during Alumina calcination

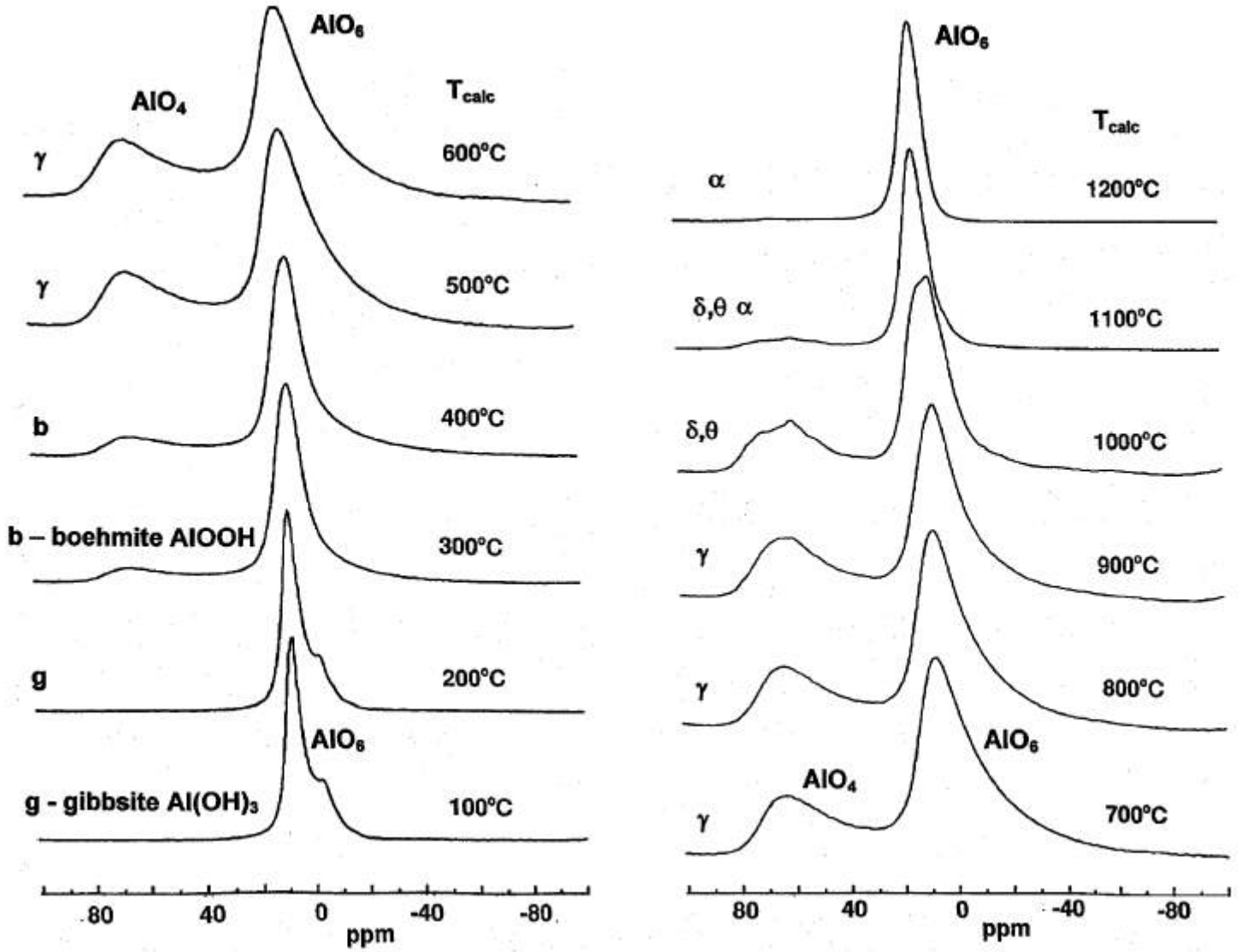

Hill et al Chem. Mater 19, 2877 (2007)

- Structures are fully relaxed

- PAW datasets with 45 Ry cutoff
  (1 mRyd/atom, 0.5 ppm in NMR chemical shifts)

- XC considered: PBE / revPBE86 / vdW-DF

- including Quadrupolar Coupling (EFG)

- spectra obtained using QuadFit code

α–alumina and θ-alumina

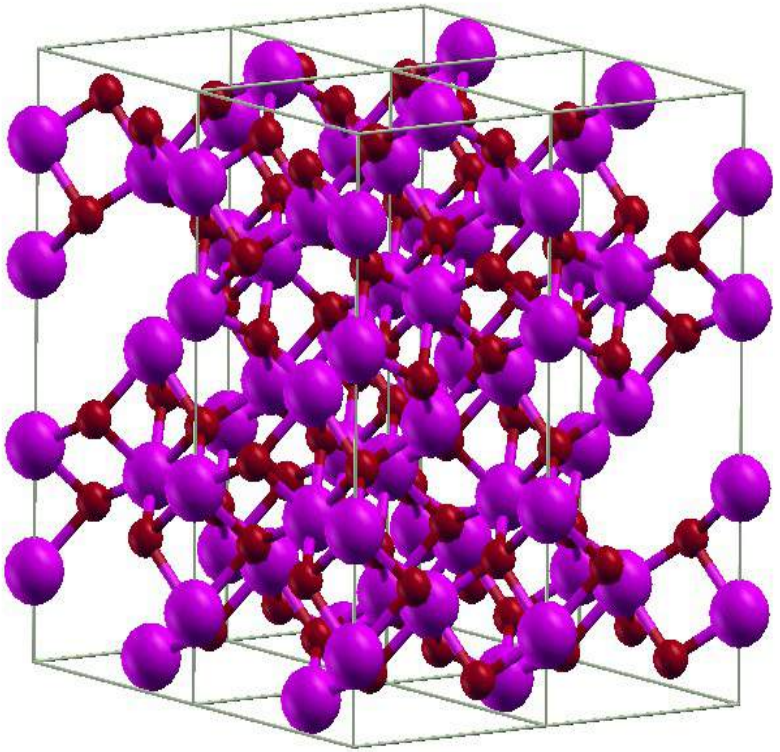

Octahedrally coordinated Al sites

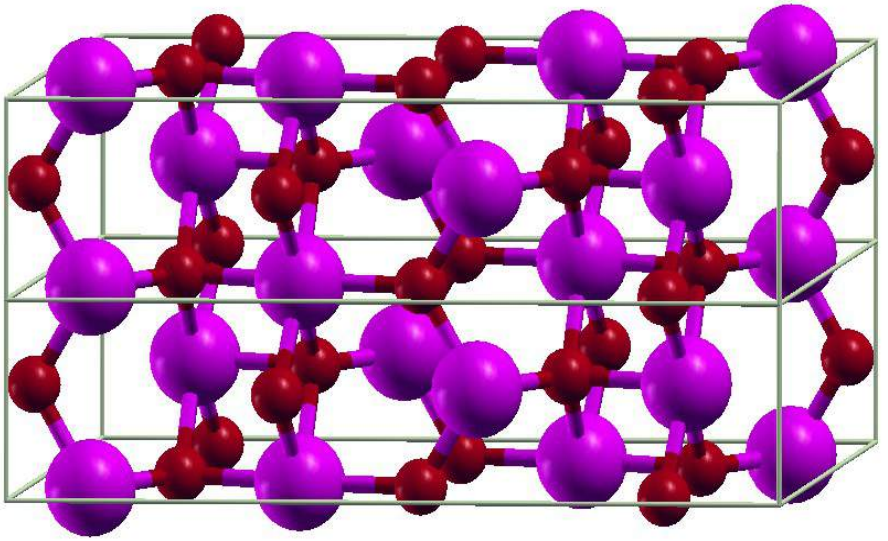

Octahedrally andTetrahedrally coordinated Al sites

α– and θ-alumina NMR spectra

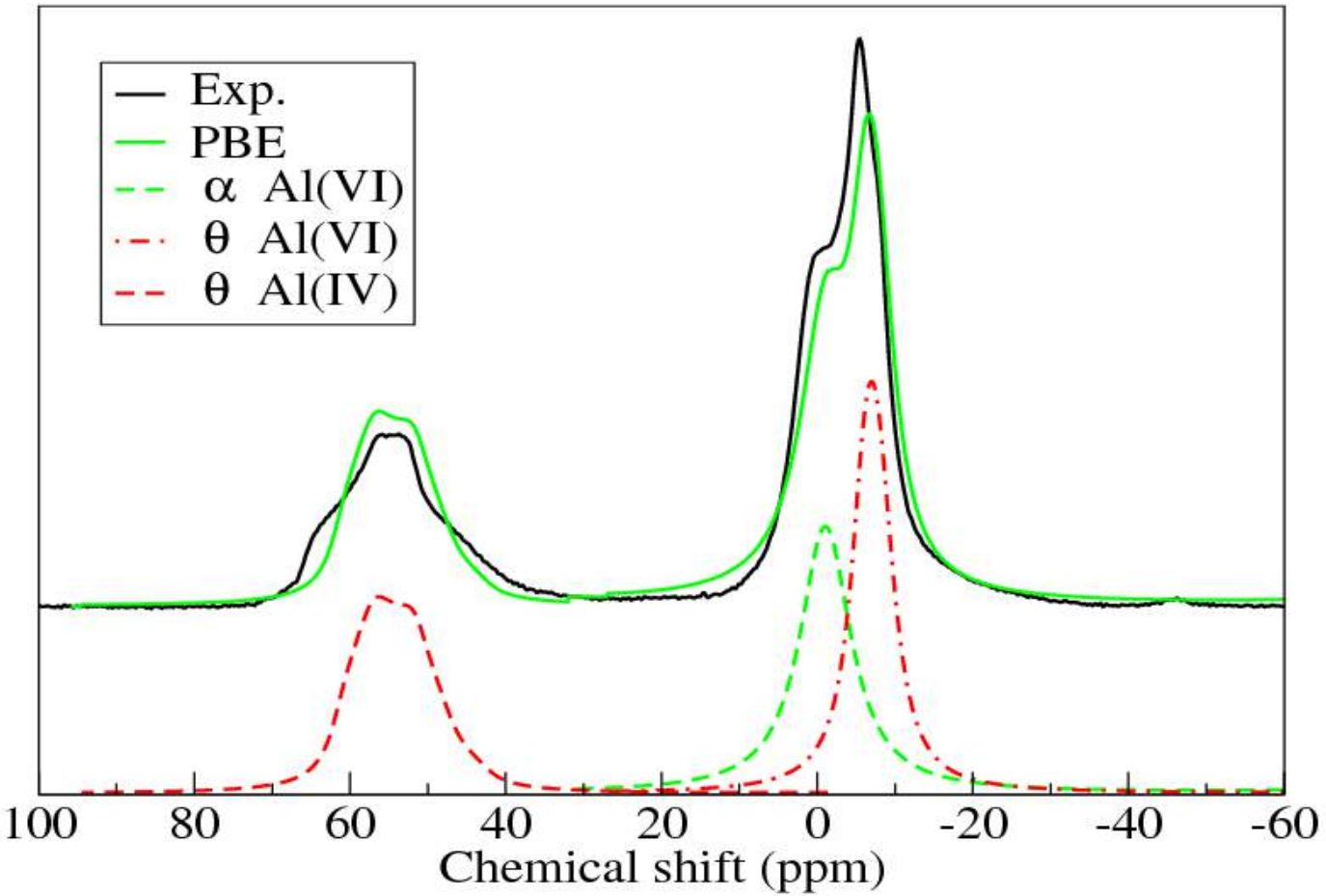

Exp: O'Dell, Savin, Chadwick, and Smith,
Solid State Nucl. Magn. Reson. **31**, 169 (2007)

Gibbsite [γ–Al(OH)3]

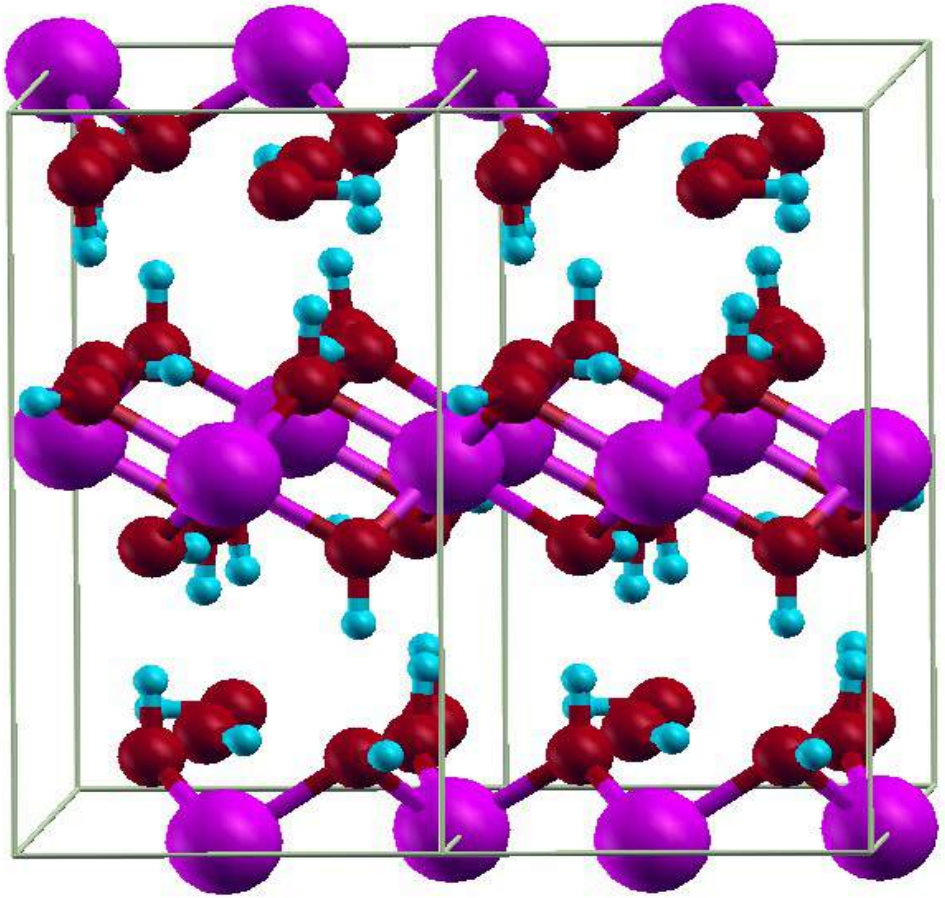

Octahedrally coordinated Al sites

Gibbsite [γ–Al(OH)3] NMR spectrum

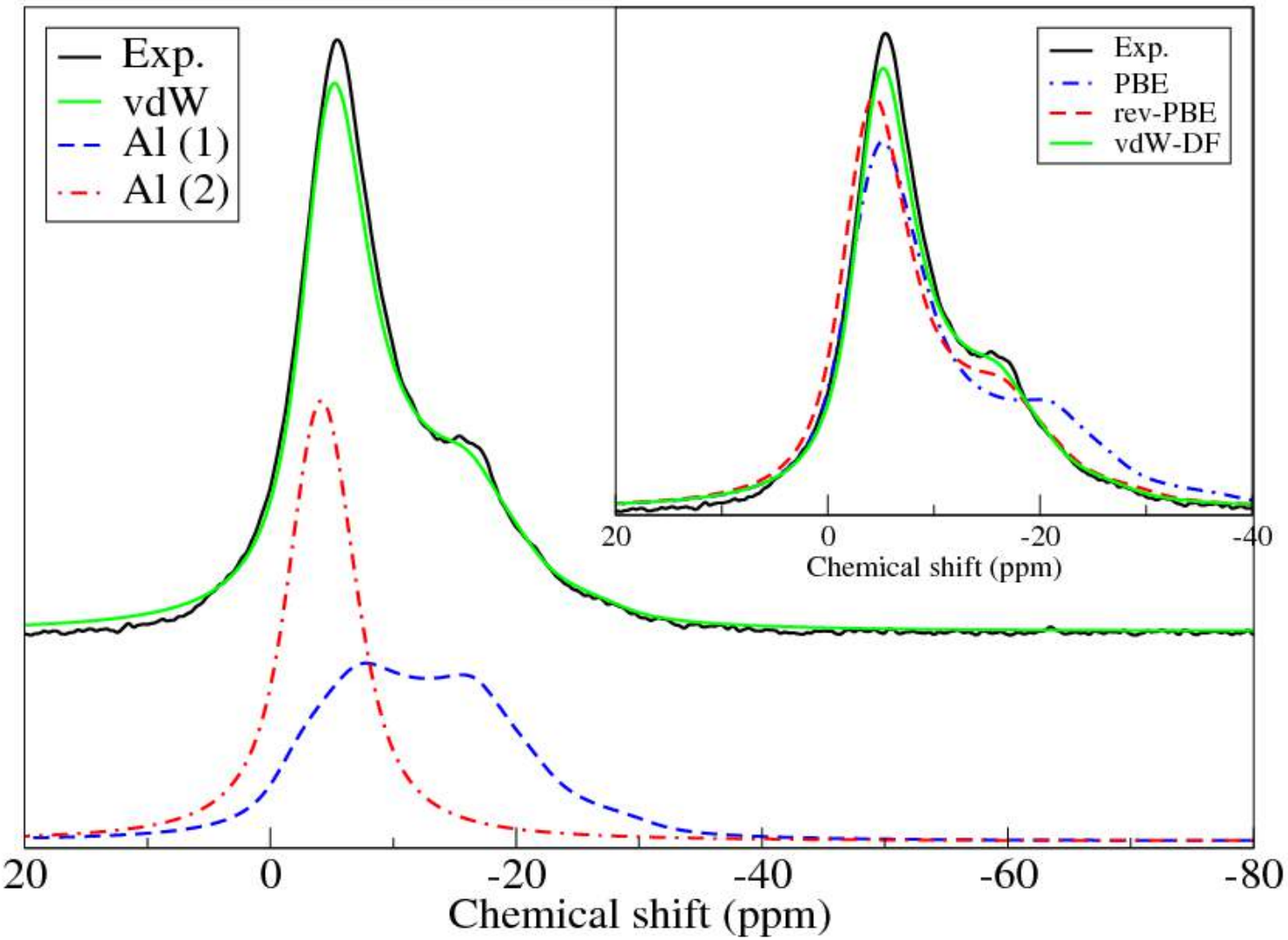

Octahedrally coordinated Al: two different H-bond networks

κ-alumina structure

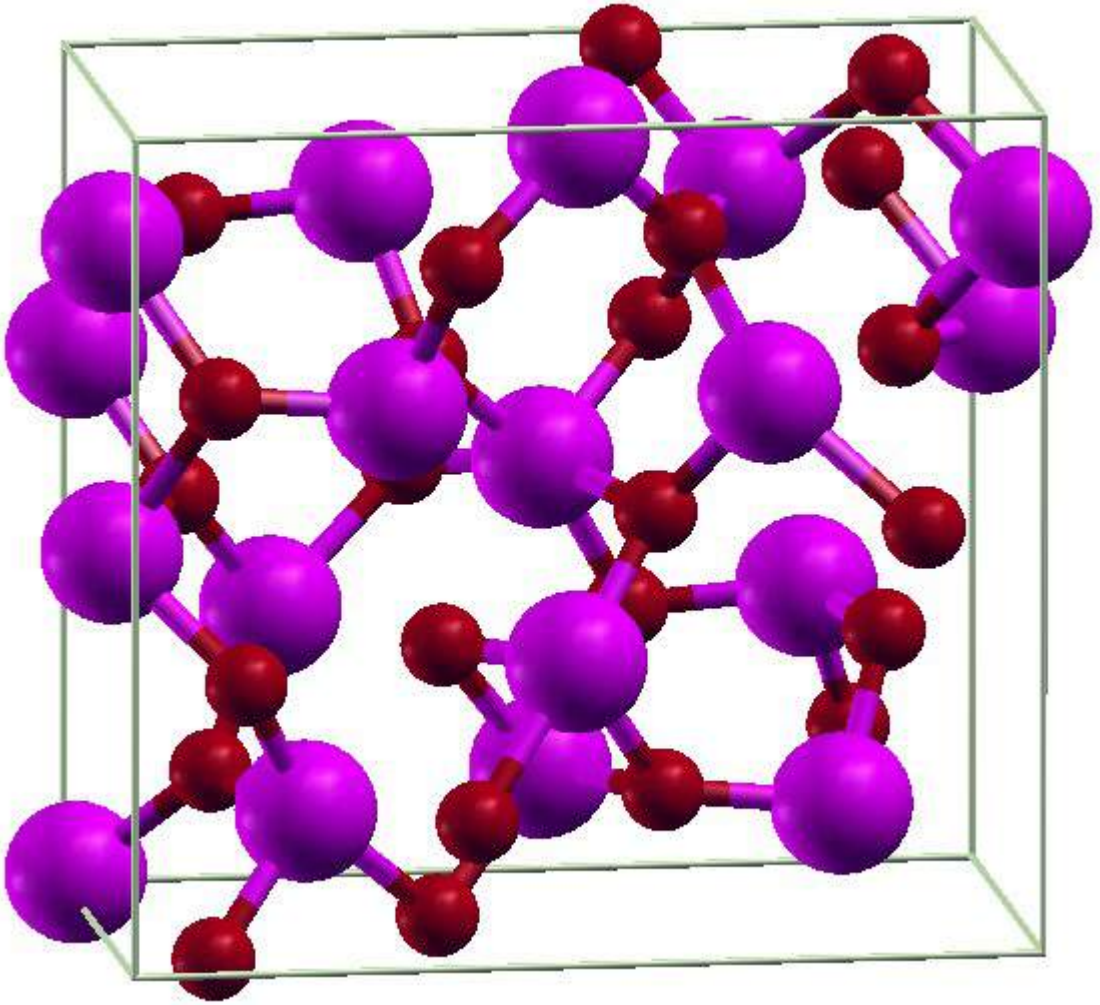

3 Octahedrally coordinated Al sites
1 Tetrahedrally coordinated Al site

κ-alumina NMR spectra

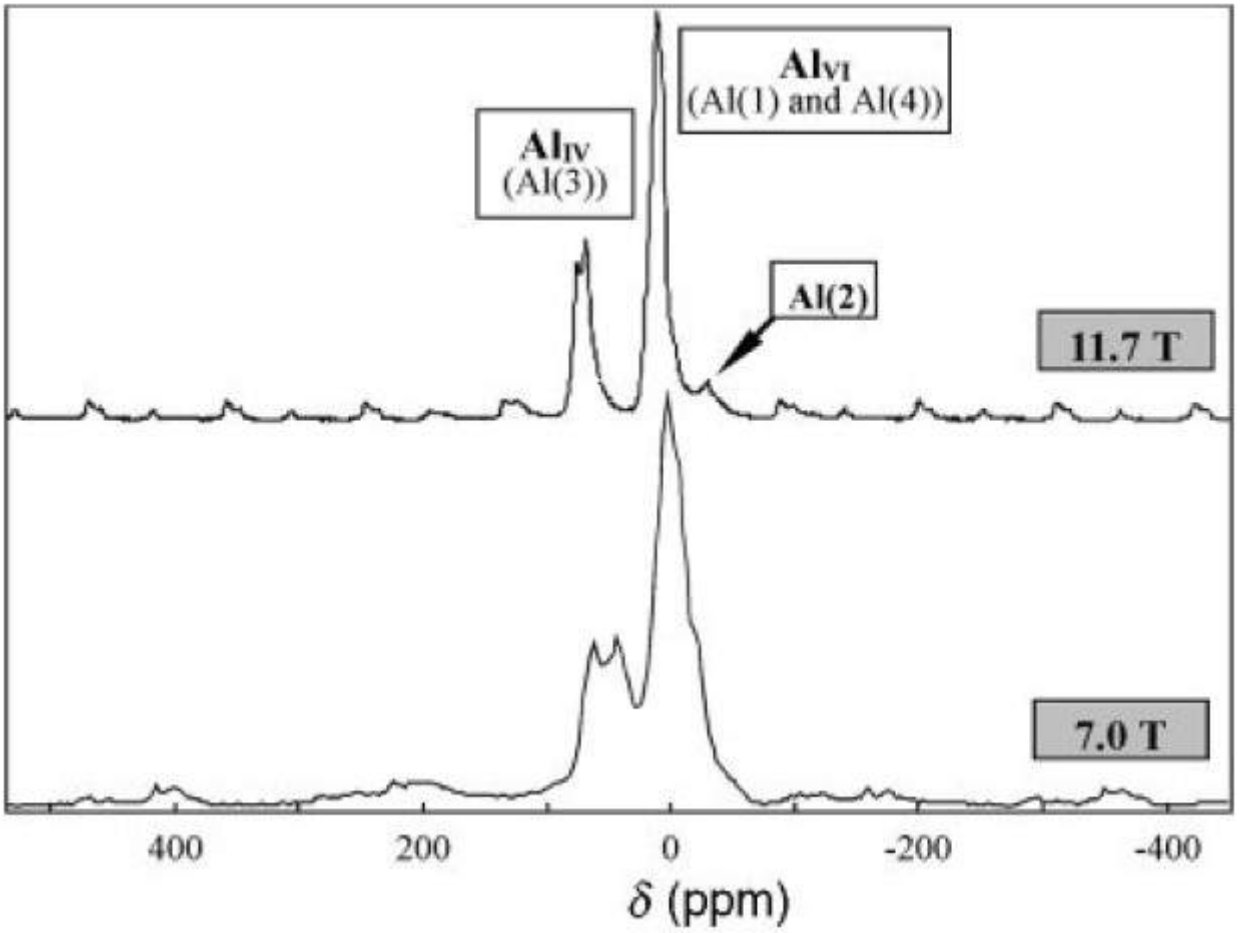

Exp: Ollivier et al. J. Mater. Chem. **7**, 1049 (1997)

κ-alumina NMR spectra

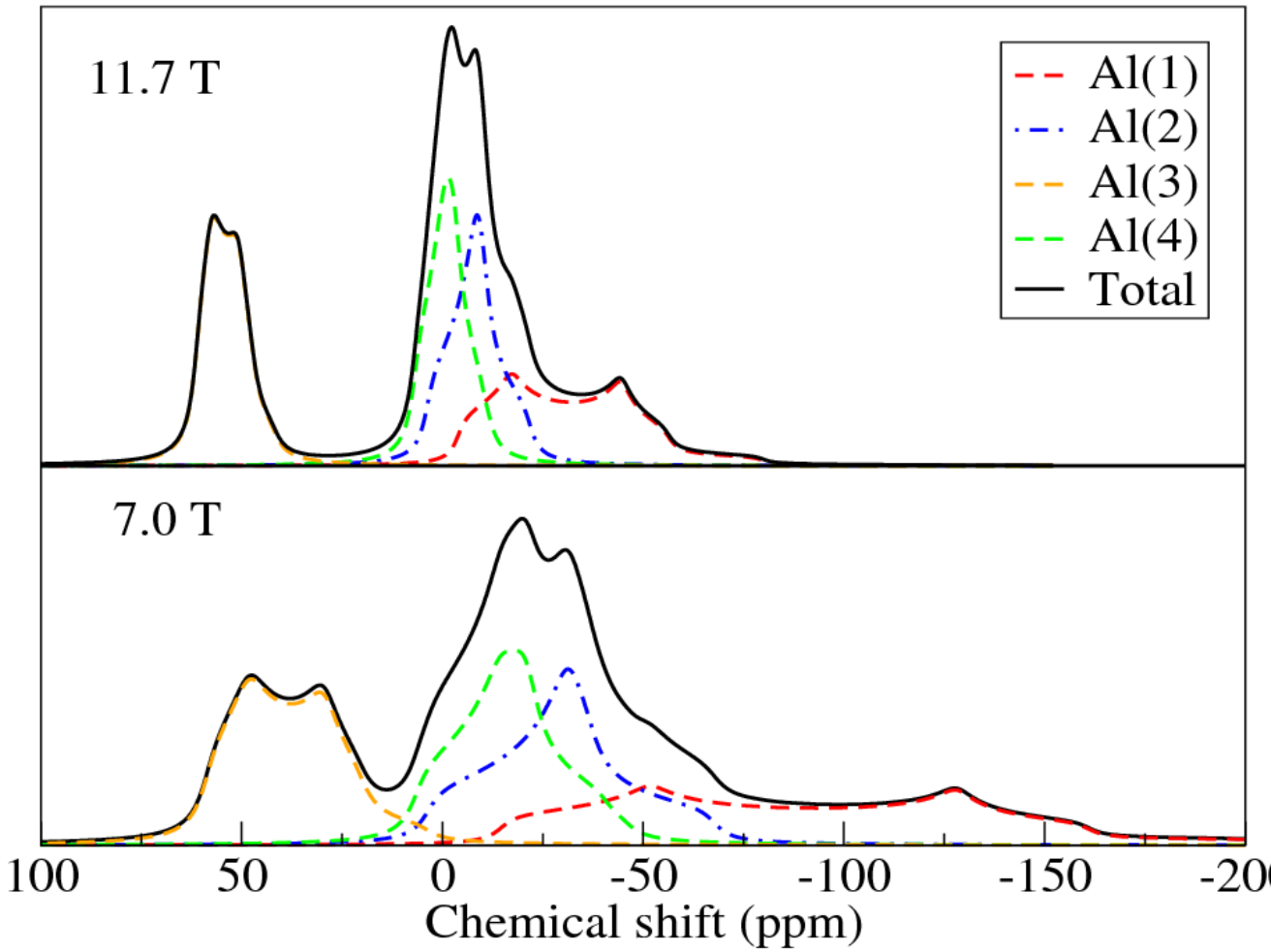

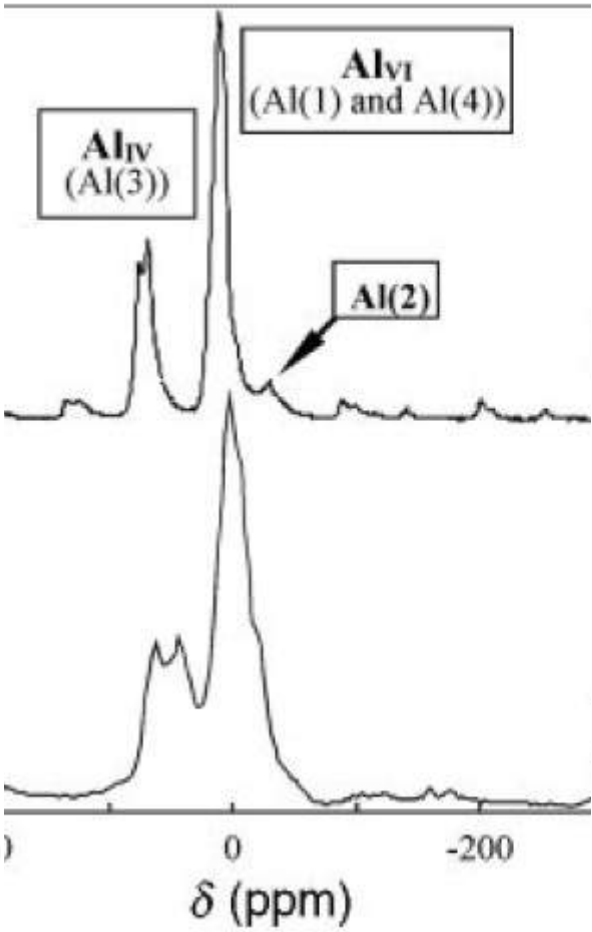

Exp: Ollivier et al. J. Mater. Chem. **7**, 1049 (1997)

γ-alumina models

(based on powder XRD)

A) Gutierrez *et al.* defective spinel model
(40 atoms – 8 formula units)

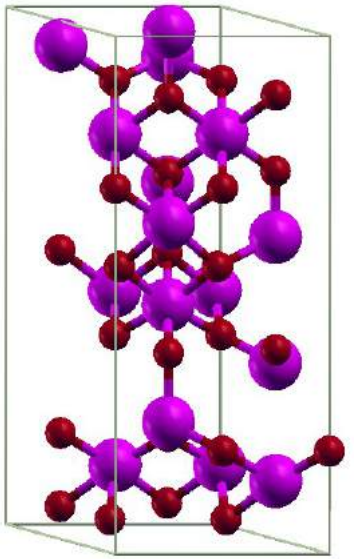

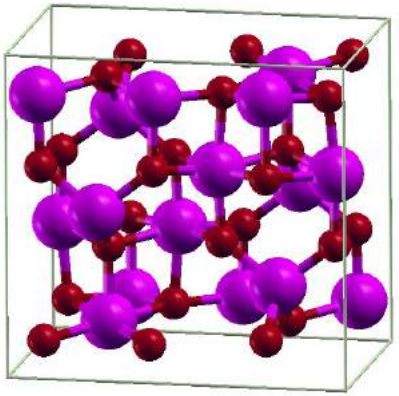

B) Krokidis *et al.* Non-spinel model
(40 atoms – 8 formula units)

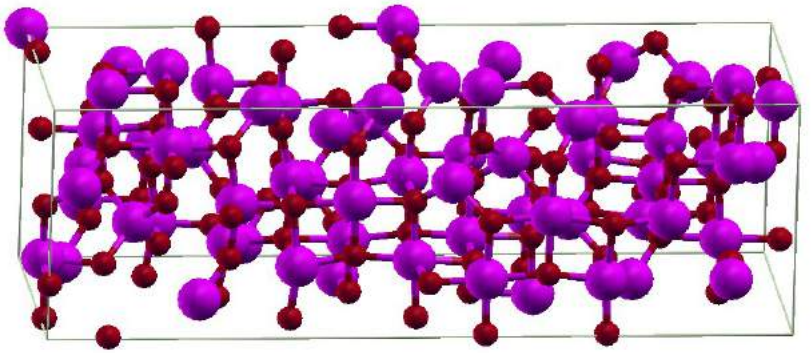

C) Paglia model Fd3m sym.
(160 atoms – 32 formula units)

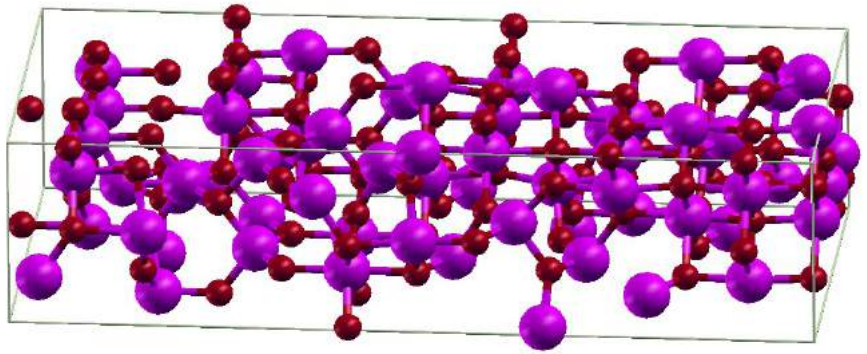

D) Paglia model I41/amd sym.
(160 atoms – 32 formula units)

gamma-alumina NMR spectra

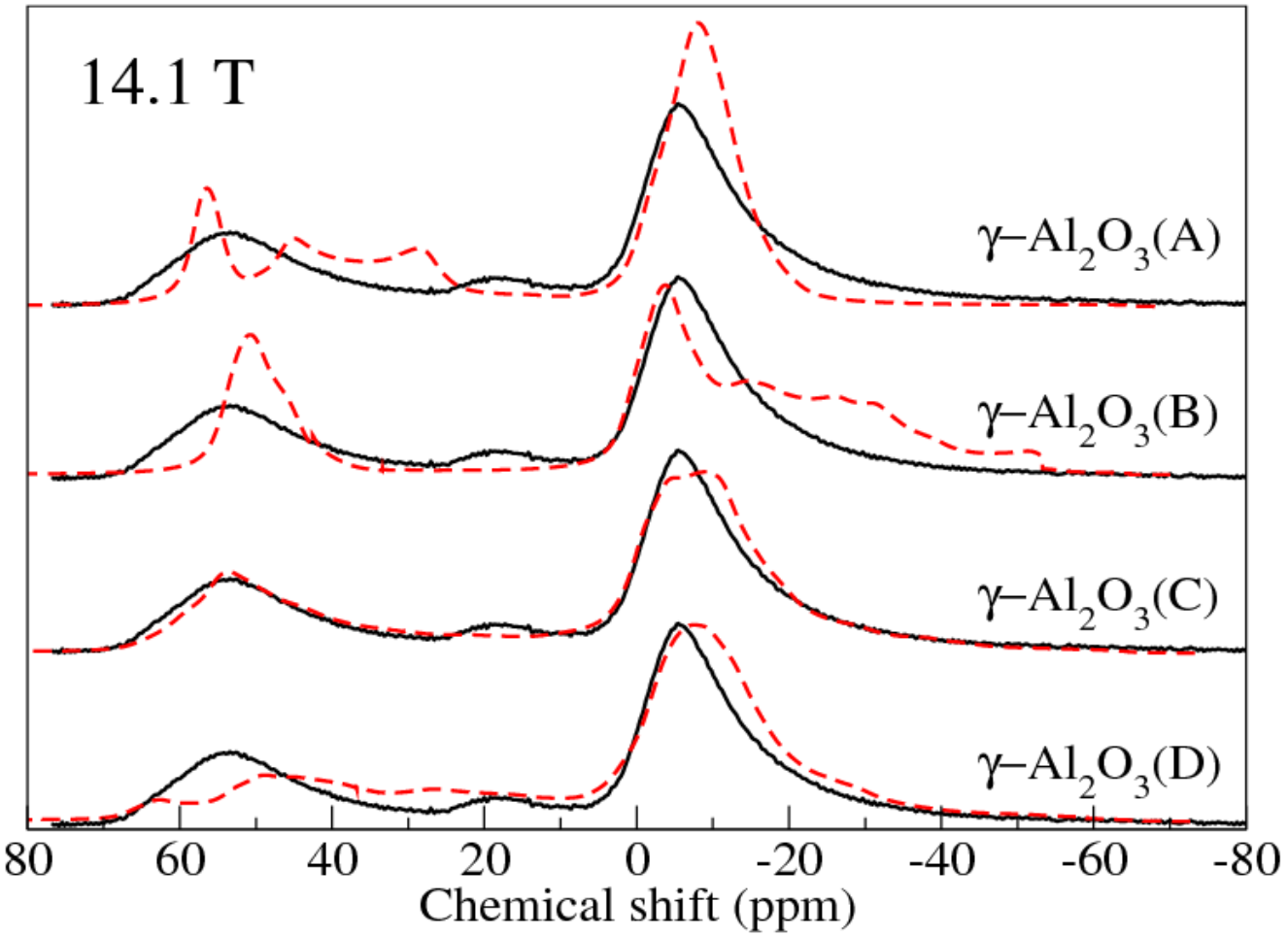

Comparison with O'Dell, Savin, Chadwick, andSmith, Solid State Nucl. Magn. Reson. **31**, 169 (2007)

gamma-alumina NMR spectra

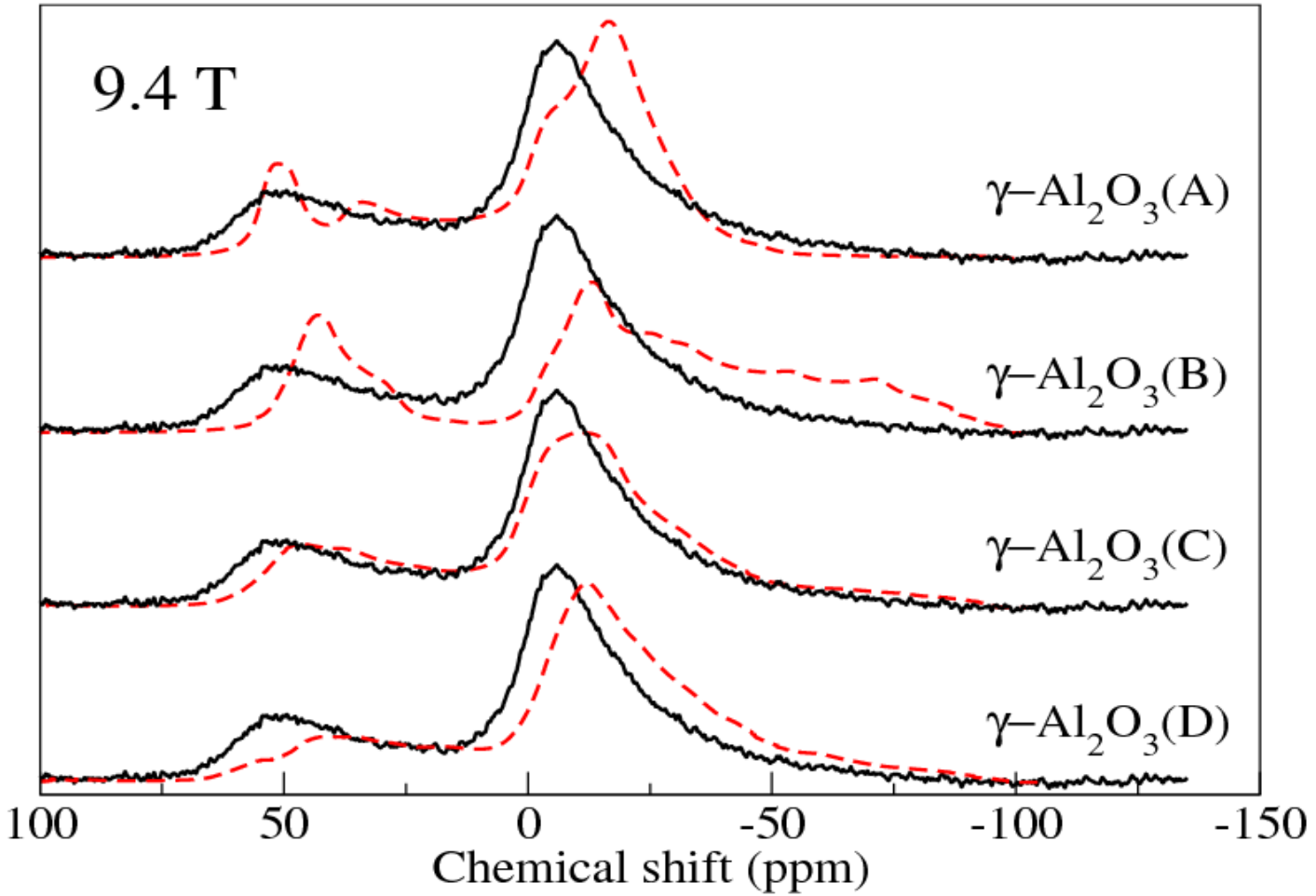

Comparison with Hill, Bastow, Celotto, and Hill, Chem. Mater. **19**, 2877 (2007).

γ-alumina models

(based on powder XRD)

A) Gutierrez *et al.* defective spinel model
(40 atoms – 8 formula units)

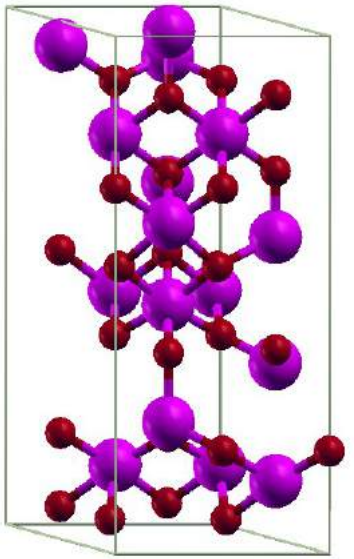

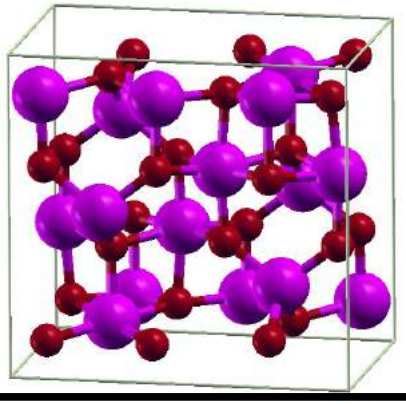

B) Krokidis *et al.* Non-spinel model
(40 atoms – 8 formula units)

C) Paglia model Fd3m sym.
(160 atoms – 32 formula units)

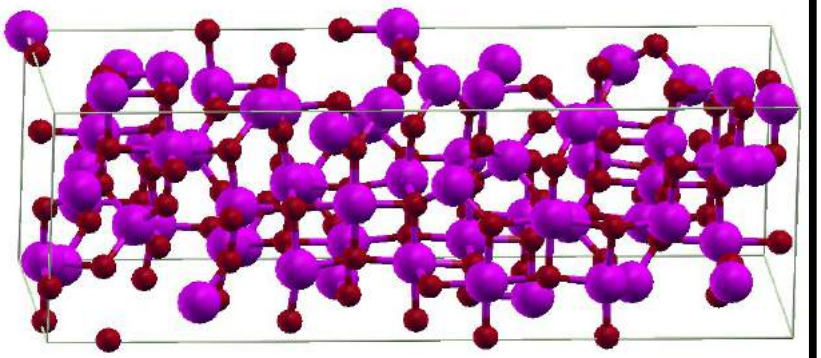

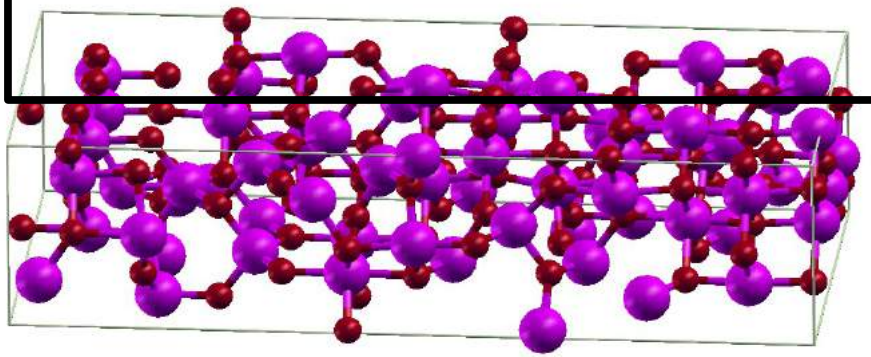

D) Paglia model I41/amd sym.
(160 atoms – 32 formula units)

Correlation of NMR chemical shifts with local Electronic Structure indicators

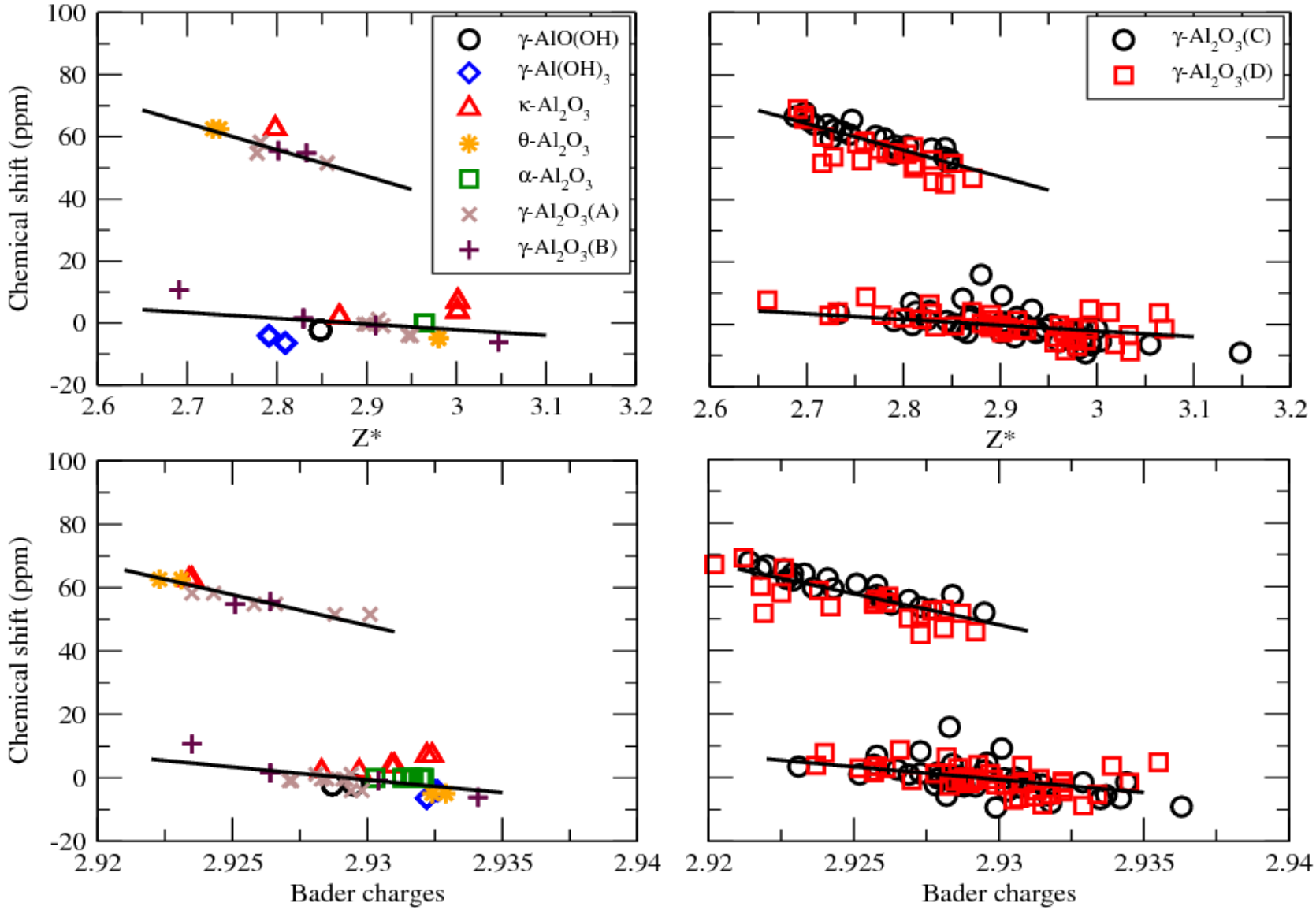

Outline

- Theory (GIPAW +PAW)

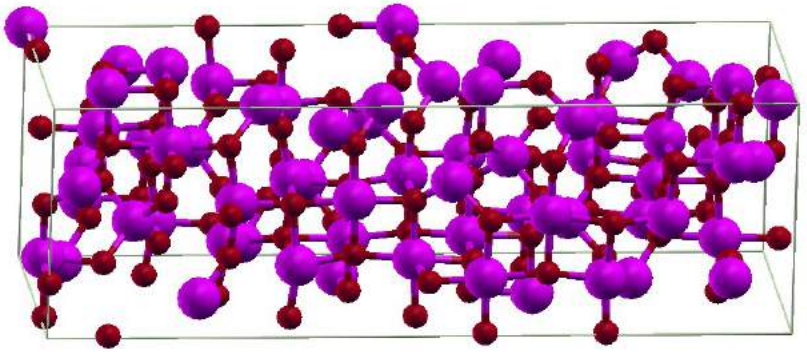

- 27Al NMR shifts of alumina and its precursors

- 13C NMR of Cholesterol Crystals

Why Cholesterol ?

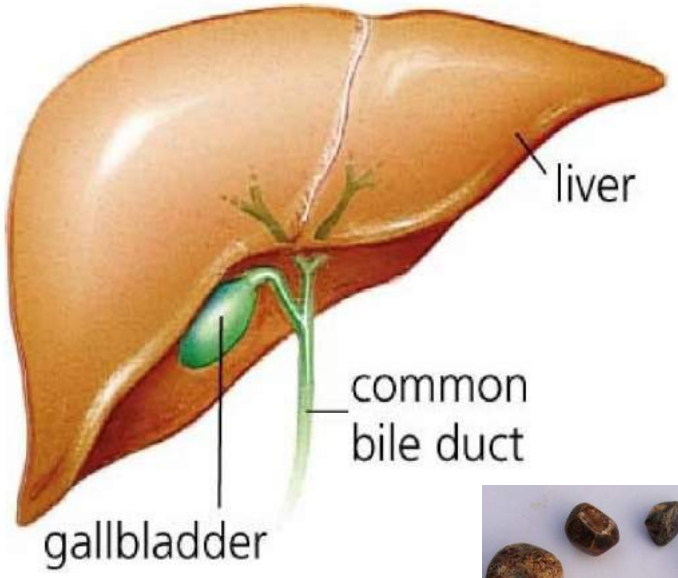

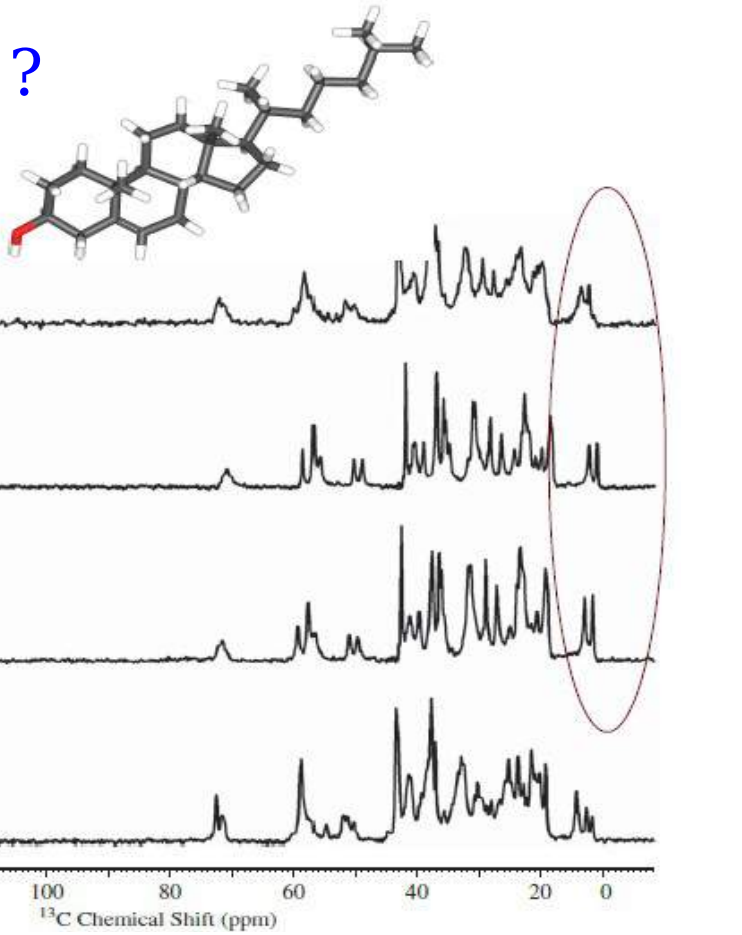

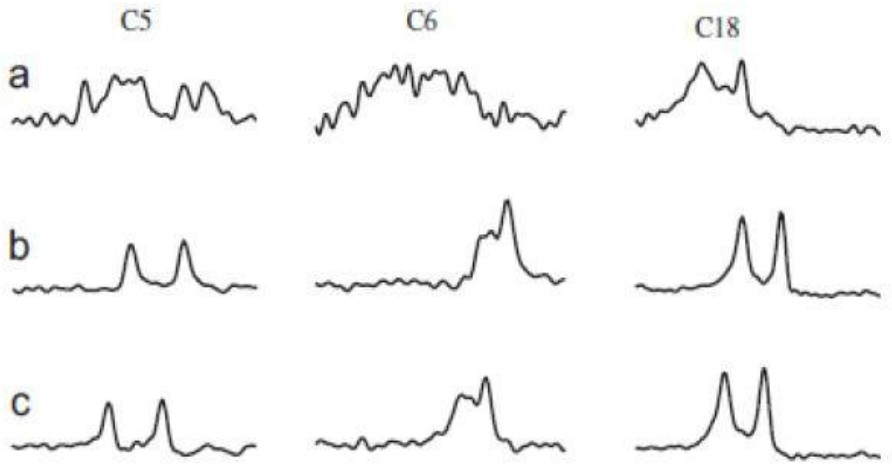

a) Gallbladder Cancer

b) Chronic Cholecystitis

c) Xantho-Granulomatous Cholecystitis

Gall stones associated to different pathologies have distinct NMR spectra.

It would be important to understand the structural differences between these stones and the underlying reasons.

Can we distinguish the NMR spectra of different Cholesterol crystalline polymorphs ?

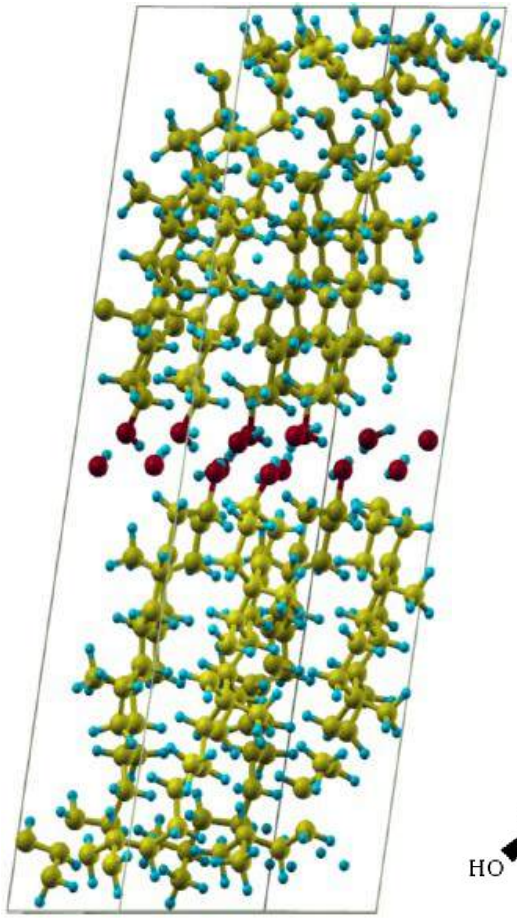

Monohydrade Cholesterol (ChM)
8 CLR +8 w molecules - 616 atoms

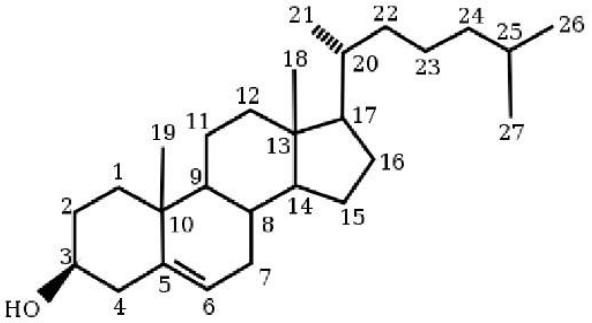

High temperature Anhydrous Cholesterol (ChAh)
16 CLR mol – 1184 atoms

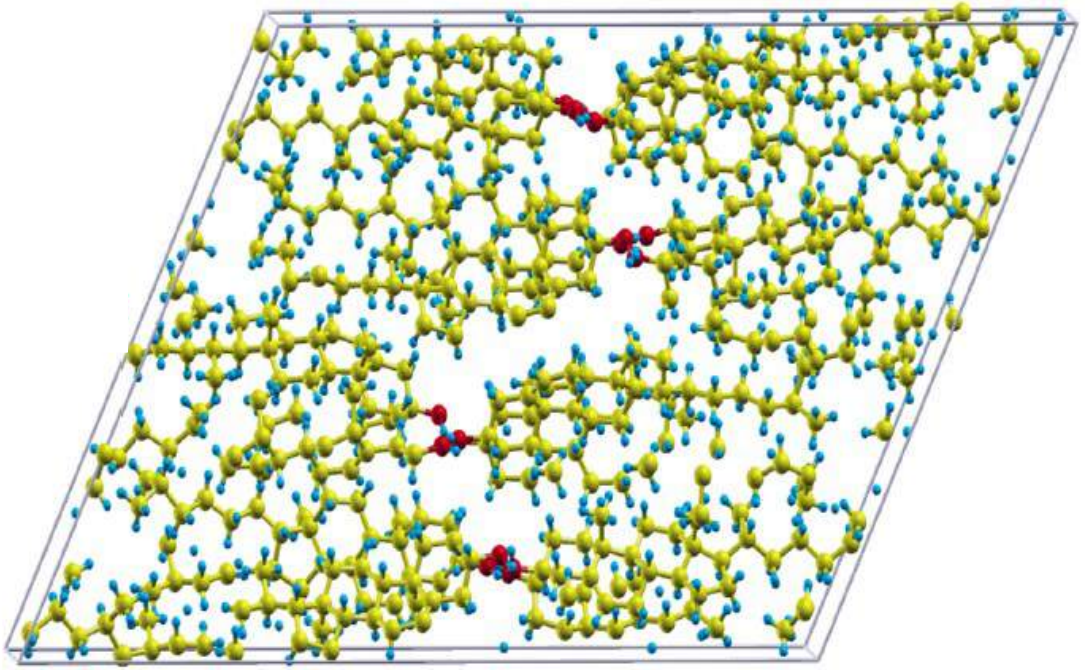

Low temperature Anhydrous Cholesterol (ChAl)
8 CLR mol – 592 atoms

(not shown)

- Structures are fully relaxed

- PAW datasets with 45 Ry cutoff
  (1 mRyd/atom, 0.5 ppm in NMR chemical shifts)

- XC considered: vdW-DF

- As GIPAW tends to over(under)-estimate the high(low)-ppm resonances with respect to Experiment for a better comparison we propose to add an environment-dependent correction:
CH0: -4.5 ppm, CH: -1.5 ppm, CH2:0.0 ppm, CH3=+2.0 ppm

Importance of accurate structural relaxation (ChM)

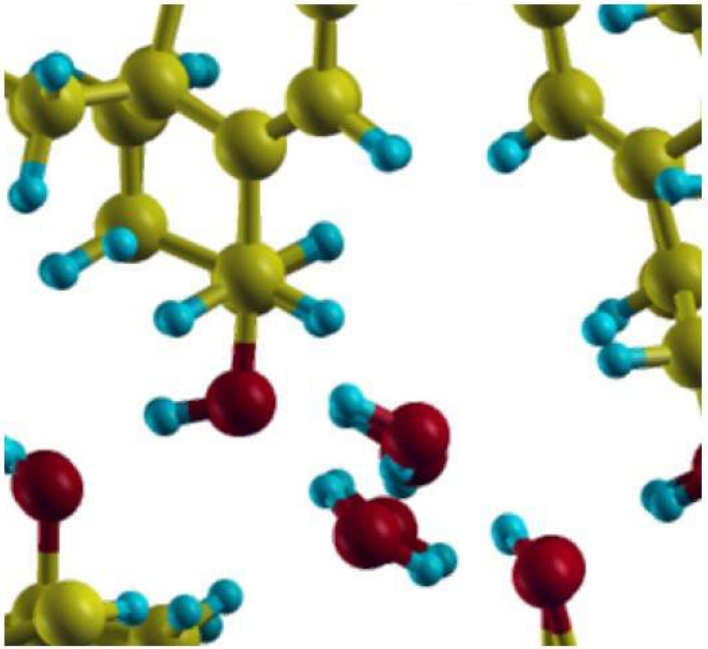

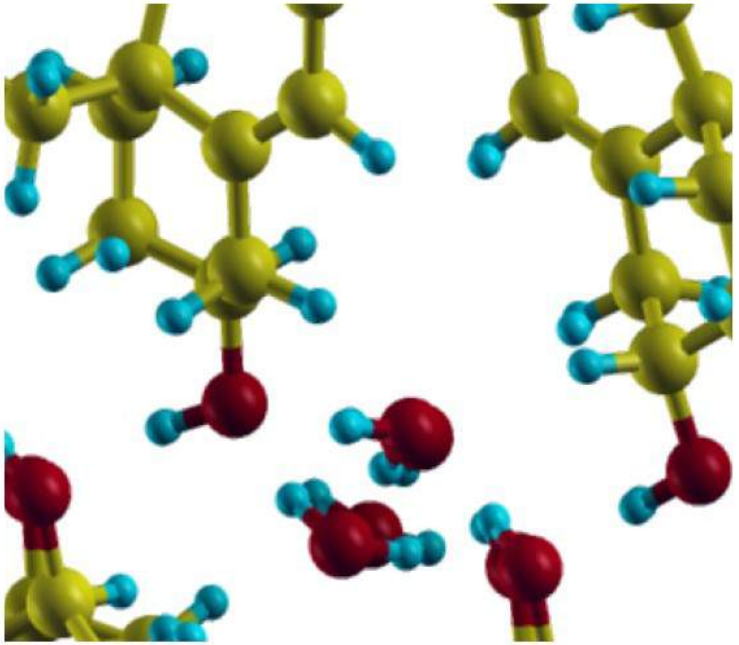

First principles

Exp + FF

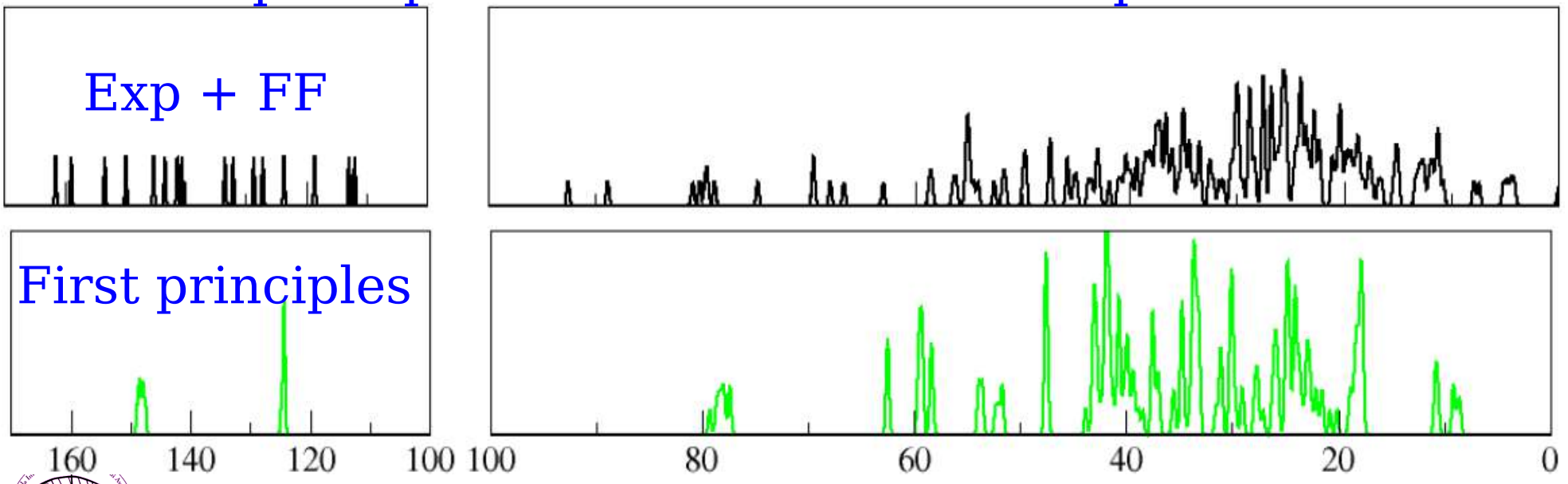

Comparison with Experimental Spectra

(E.Kucukbenli, K.Sonkar, N. Shina, SdG, JPCA 2012)

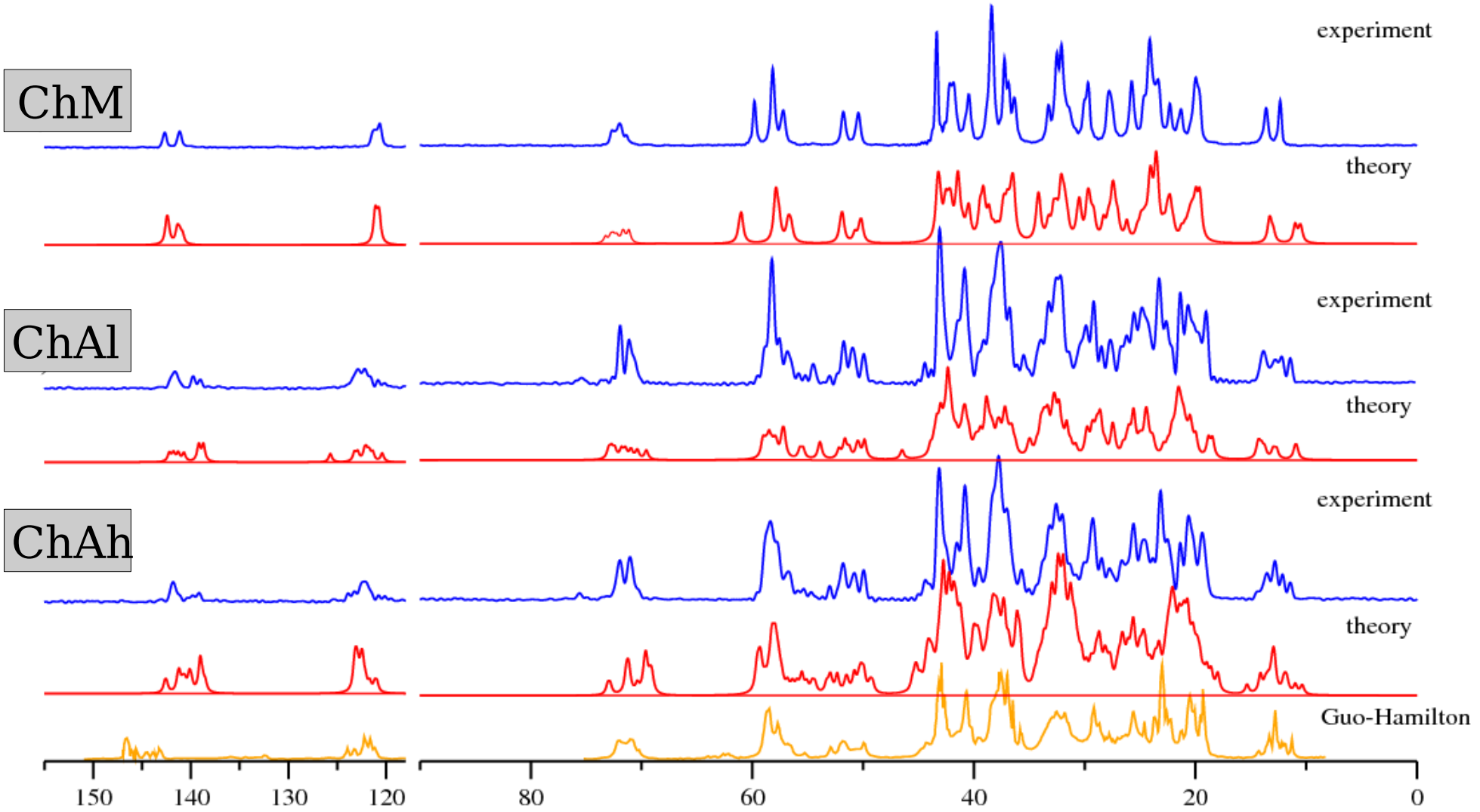

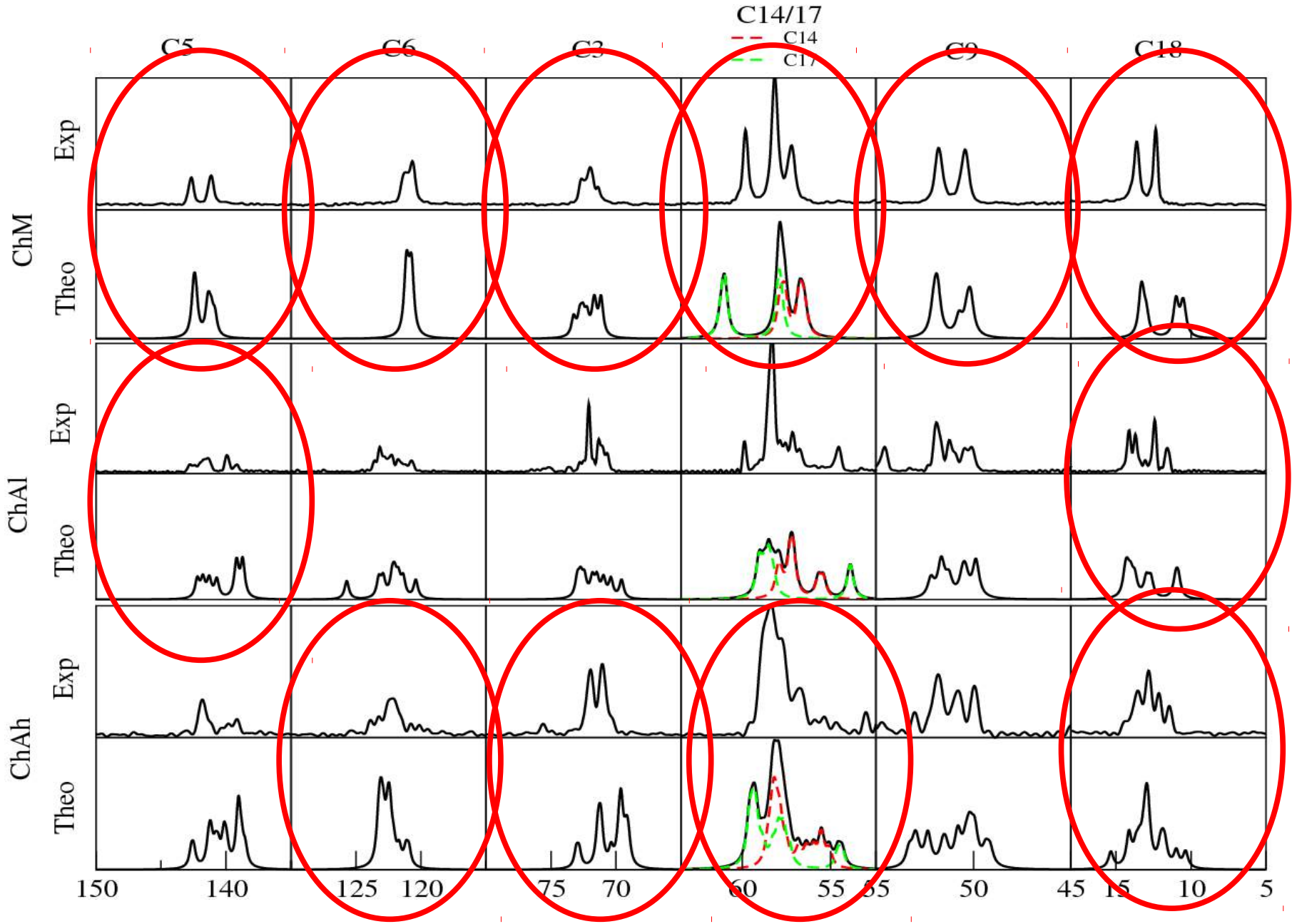
C14/17
C14
C17
C5
C6
C3
C9
C18
ChM
ChAl
ChAh
Exp
Theo
150
140
125
120
75
70
60
55
55
50
45
15
10
5

Peak assignement in ChM

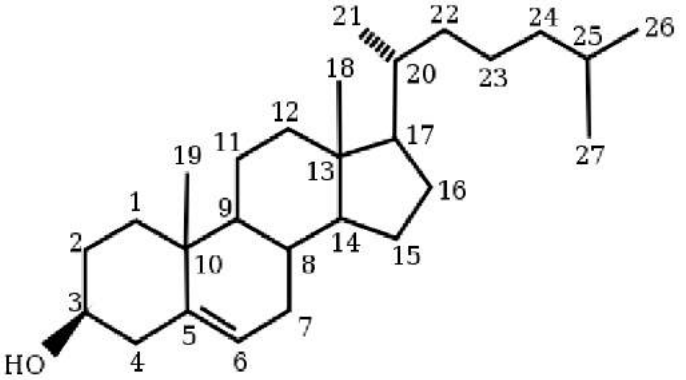

a) ChM-Exp

C17
C14
C17
C14
C9
C13
C12
C4
C20
C1
C10
C20
C7
C8
C15
C11
C16
C2
C27
C21
C19
C18
C22
C24
C25
C23
C26

b) ChM-Theory

60
50
40
30
20
10

Spectral editing

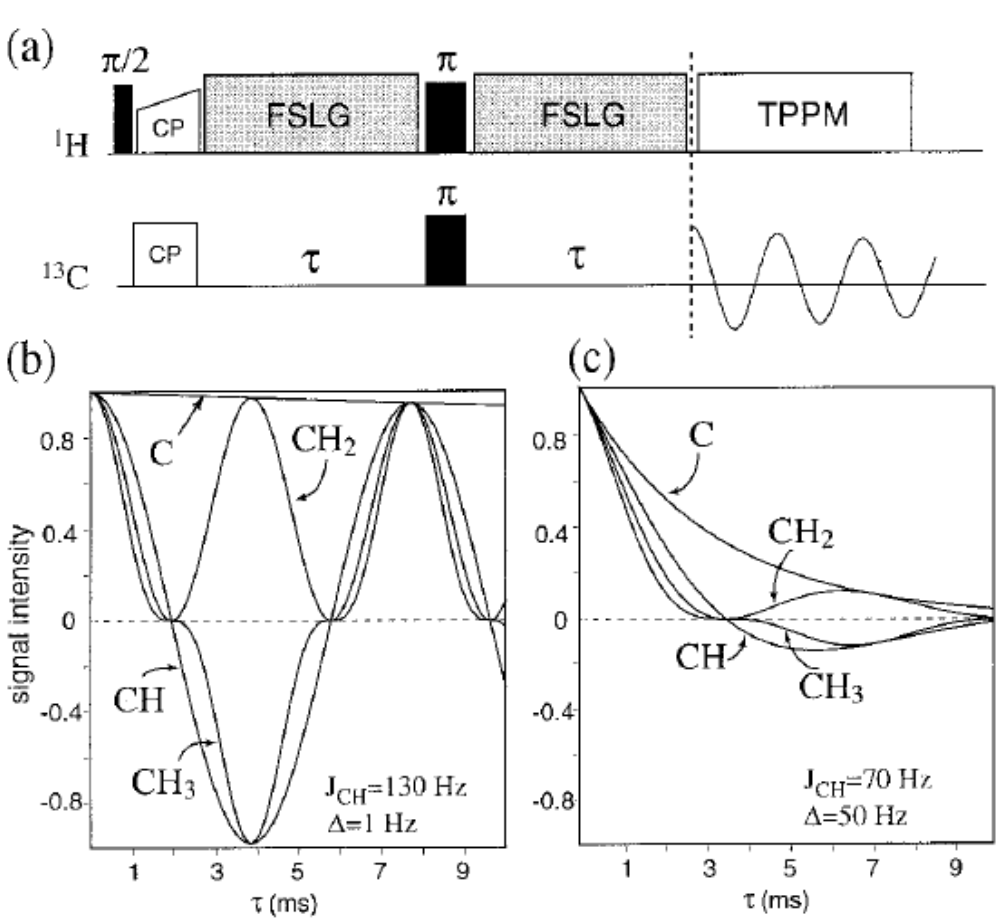

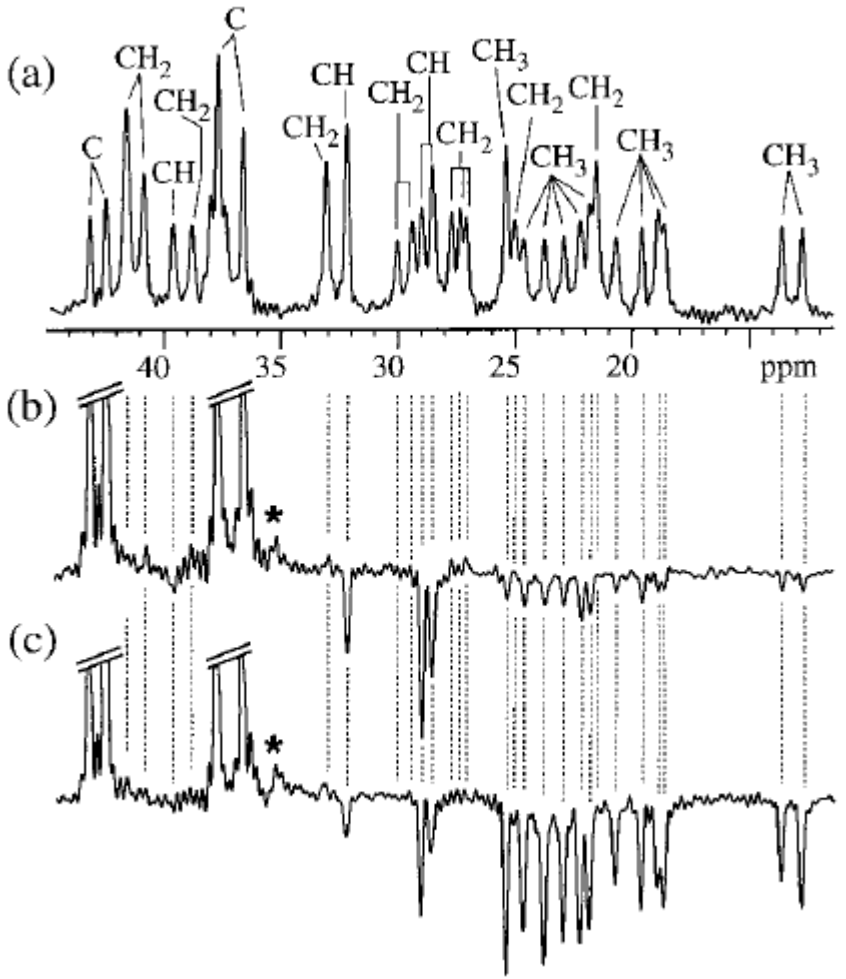

ChAl Spectral editing

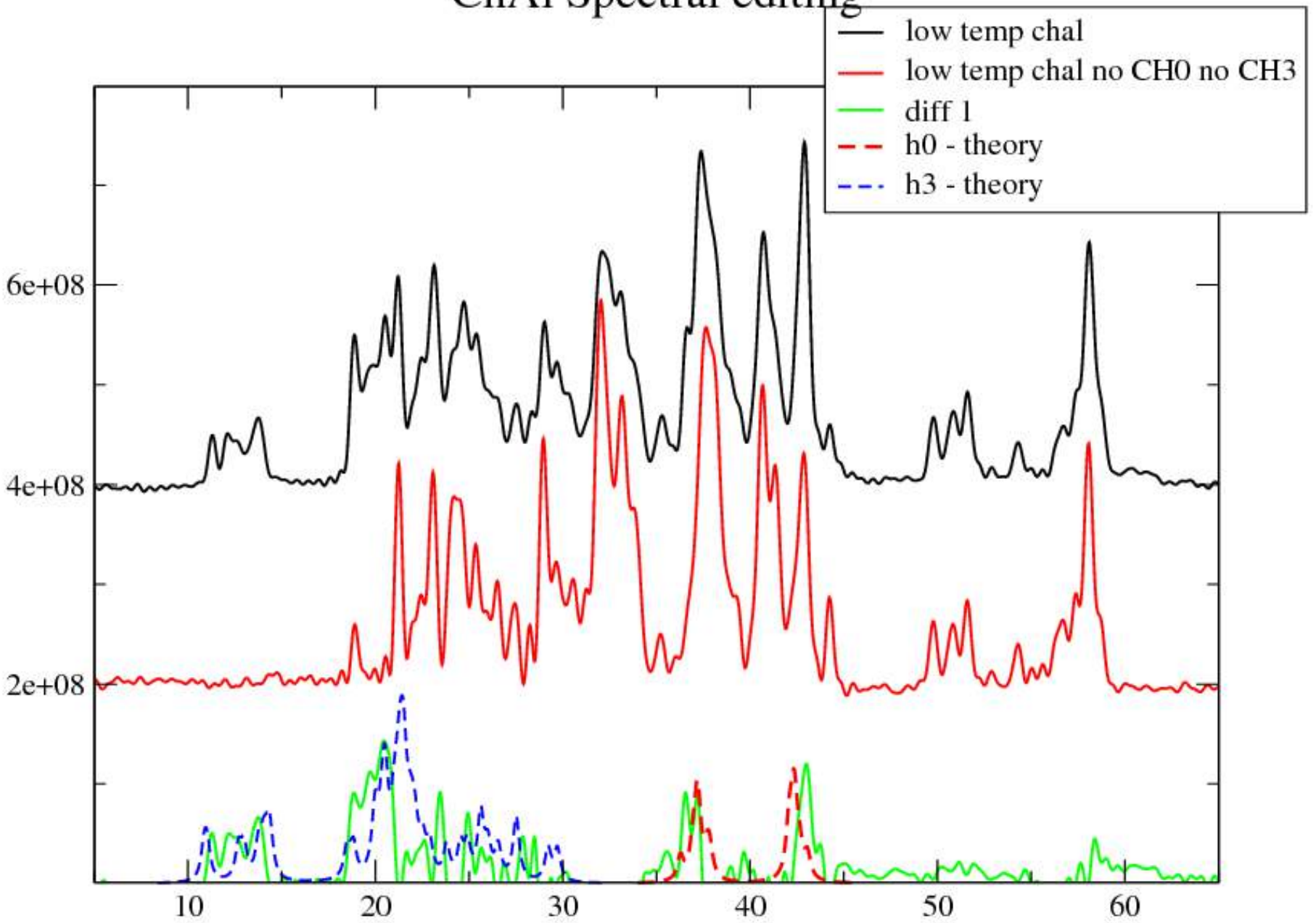

Summary

- Theory:
  GIPAW +PAW fully implemented

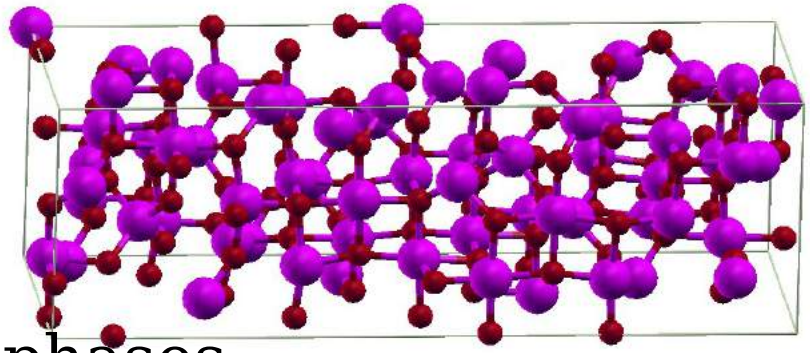

- ^{27}Al NMR shifts of alumina and its precursors

Good agreement for well knonw phases
Calculations support Paglia's Fd3m model for γ-alumina

- ^{13}C NMR of Cholesterol Crystals
  Calculations reproduce the main features of the spectra and are able to distinguish different polymorphs
  It is possible to provide a complete peak assignment, confirmed with spectral editing exp.

Credits

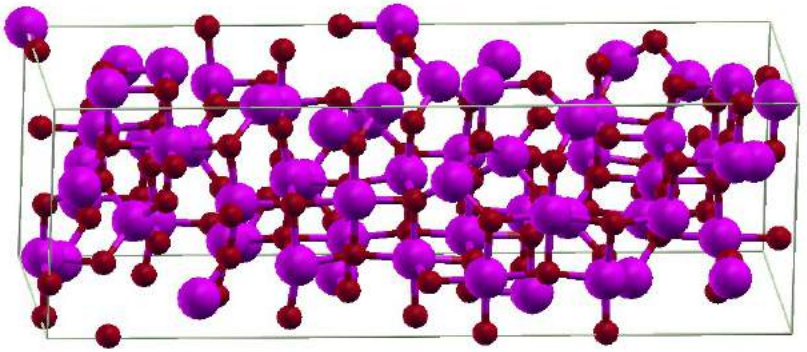

- Theory (GIPAW +PAW)

  Emine Kucukbenli

- ^{27}Al NMR shifts of alumina and its precursors

  Ary Ferreira, Emine Kucukbenli, Alexandre Leitao
  UFJF Brasil - BR PETROBRAS

- ^{13}C NMR of Cholesterol Crystals

  Emine Kucukbenli, Kanchan Sonkar,
  Neeraj Shina
  Centre of Biomedical Magn. Resonance,
  Lucknow, India

ζ-Glycine: Insight into the mechanism of a polymorphic phase transition

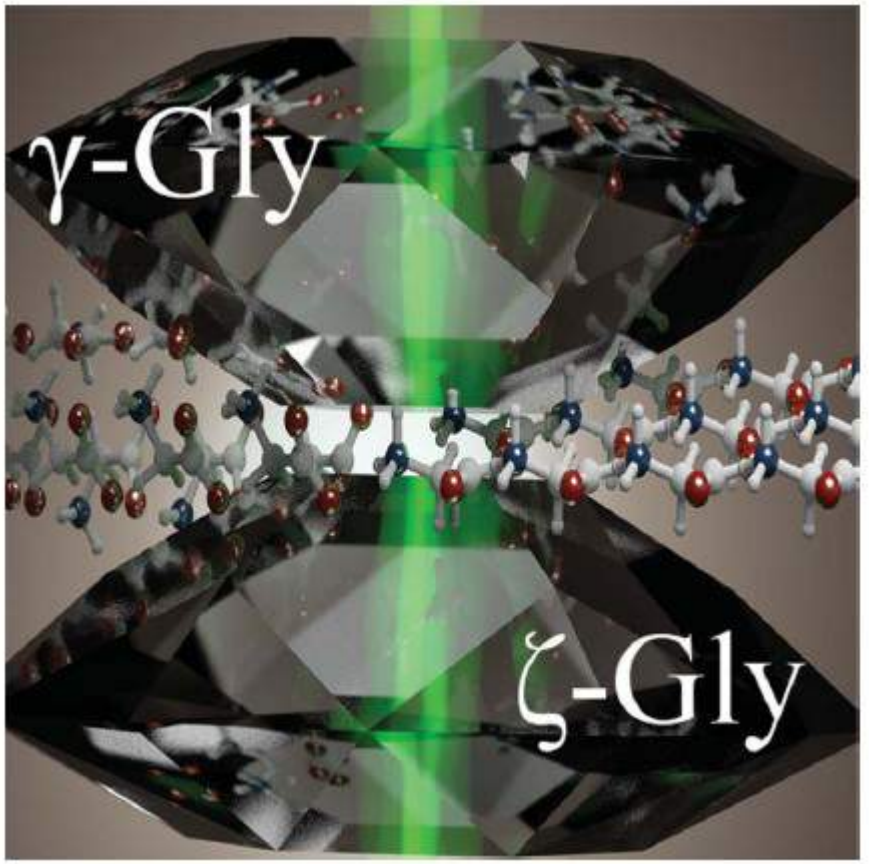

Glycine

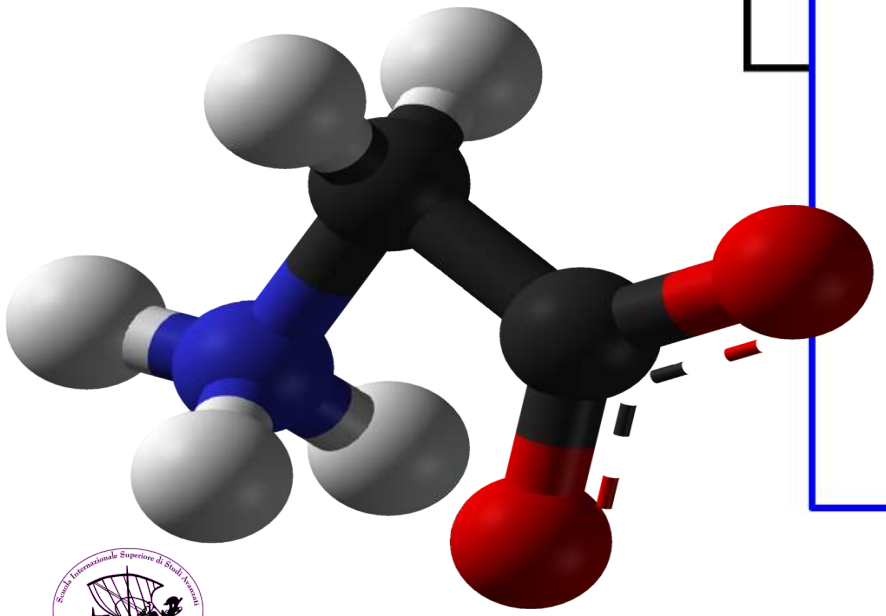

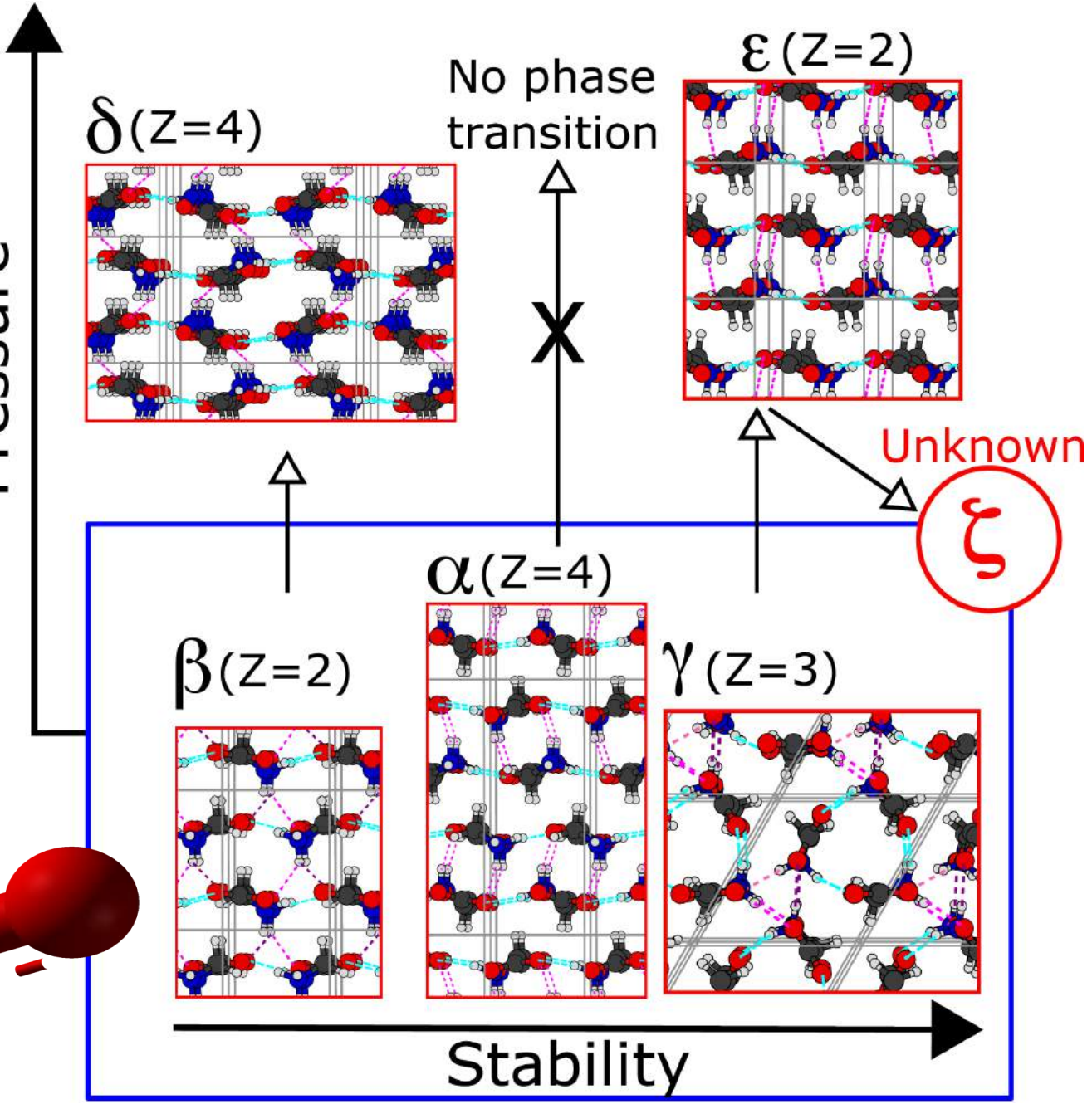
Pressure
δ (Z=4)
No phase transition
ε (Z=2)
Unknown
ξ
α (Z=4)
β (Z=2)
γ (Z=3)
Stability

Is CSP a formidable problem?

- CSP problem: Name a chemical or stoichiometric formula; find the (local) minima of the free energy landscape under given thermodynamic conditions (often at certain T,P)
- “What is the most stable structure of glycine at ambient conditions?” “What is the carbon structure that is stable at very high pressures”
- Challenges:
  - A very vast space of possibilities.
  - Free energy landscape is very expensive to obtain accurately

How to tackle CSP?

Explore: Use smart algorithms to explore as much of the landscape as possible

Molecular dynamics / Monte Carlo walkers

- Simulated annealing
- Metadynamics
- Basin hopping
- Minima hopping
- Genetic algorithm

Genetic algorithm

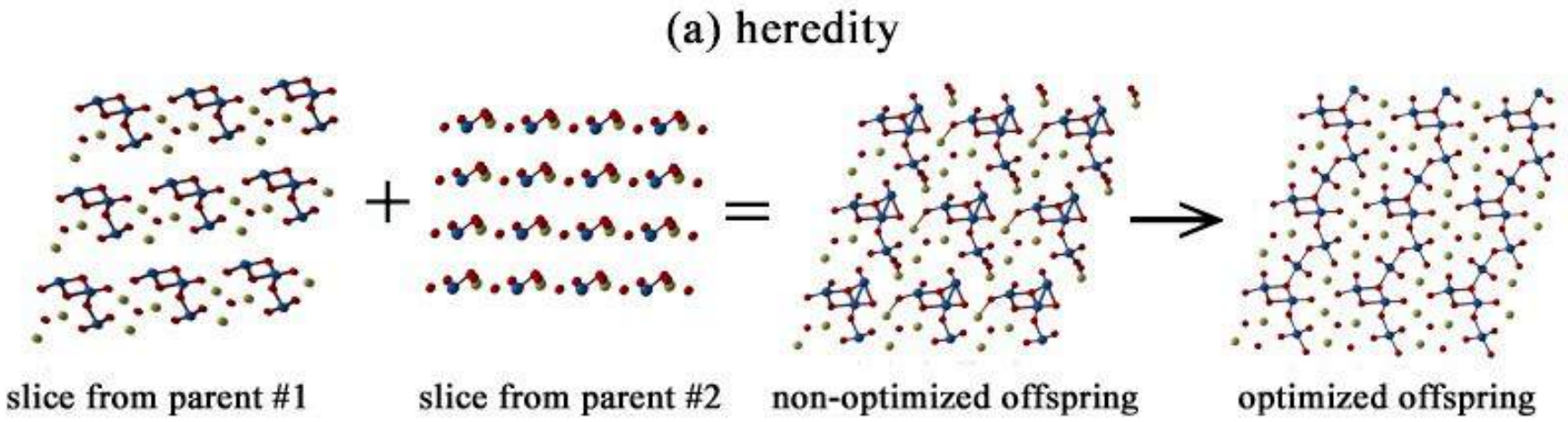

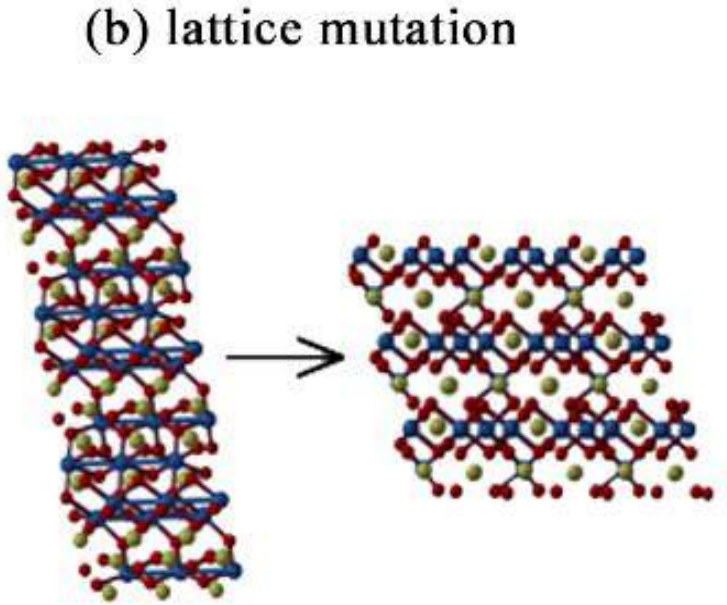

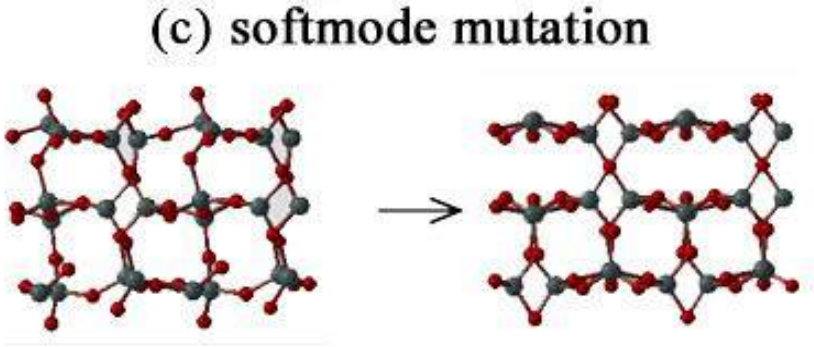

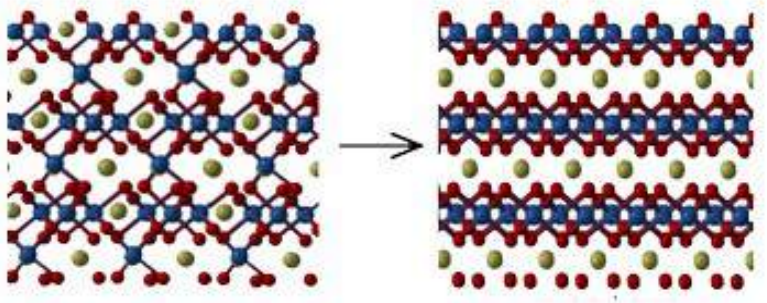

USPEX operations


USPEX

+


QUANTUM ESPRESSO

+

+ vdWDF + clustering

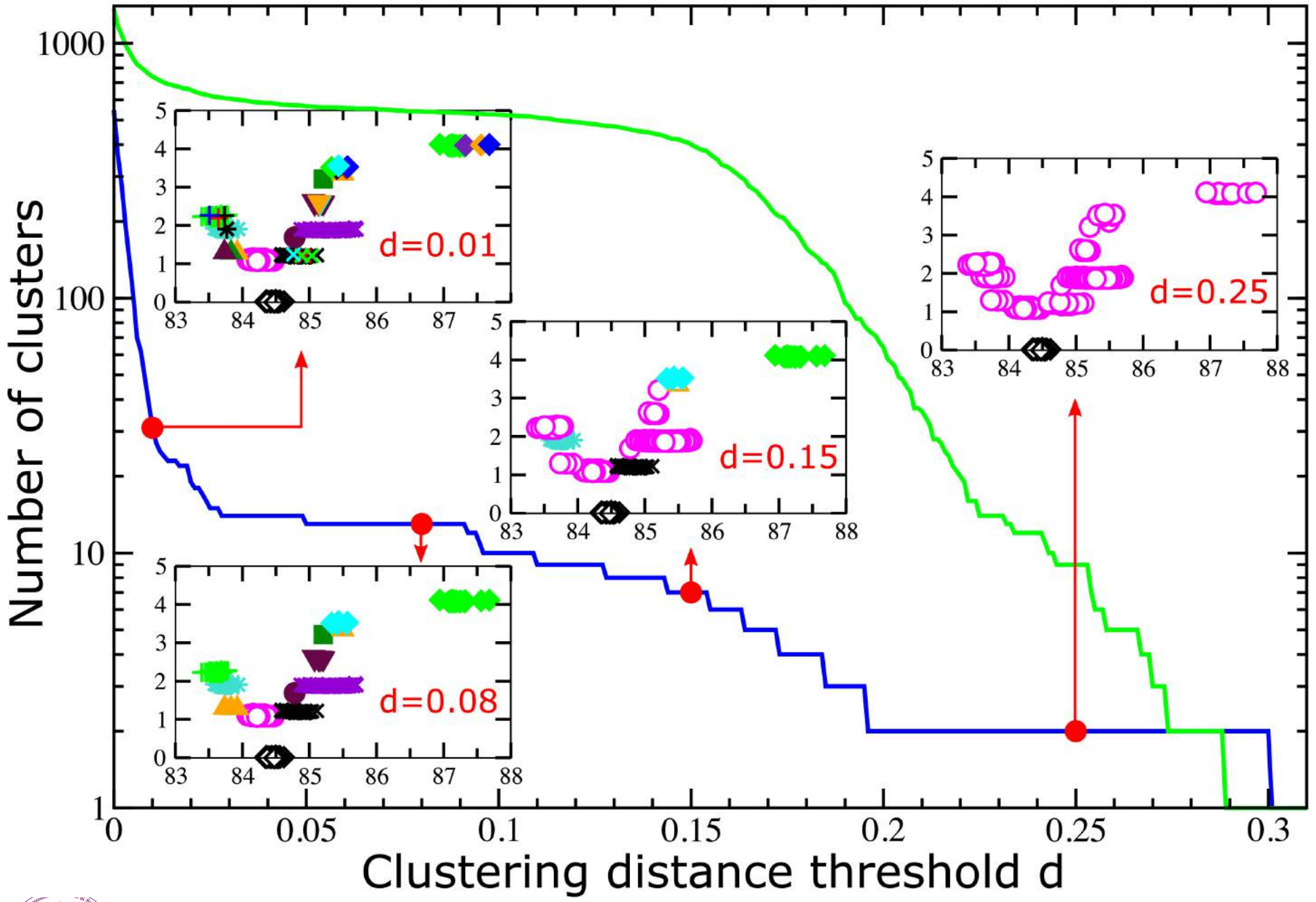
Number of clusters
1000
100
10
1
0
0.05
0.1
0.15
0.2
0.25
0.3
Clustering distance threshold d
d=0.01
d=0.08
d=0.15
d=0.25

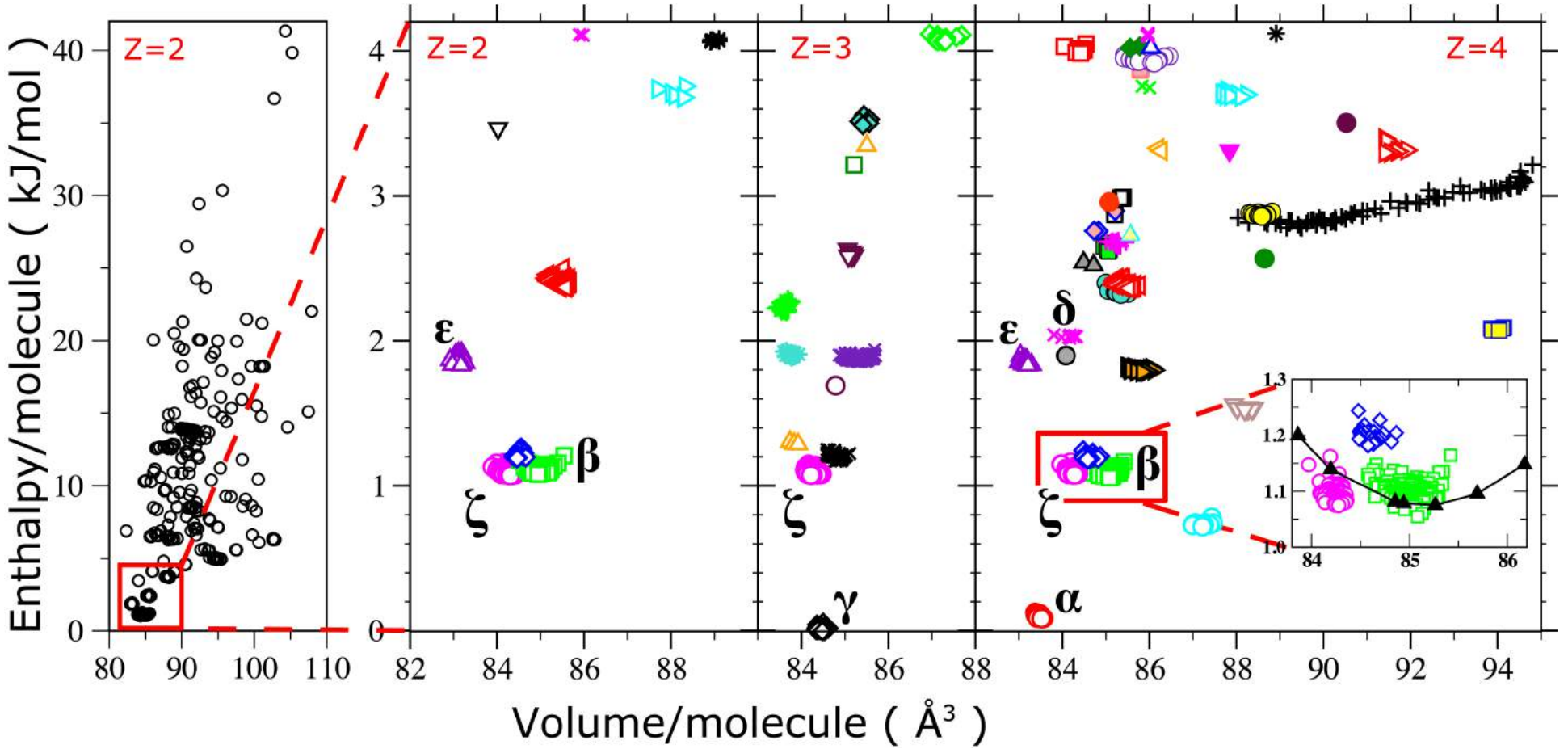
Z=2
Z=2
Z=3
Z=4
Enthalpy/molecule (kJ/mol)
Volume/molecule (Å³)
α
β
γ
δ
ε
ζ

ζ–phase

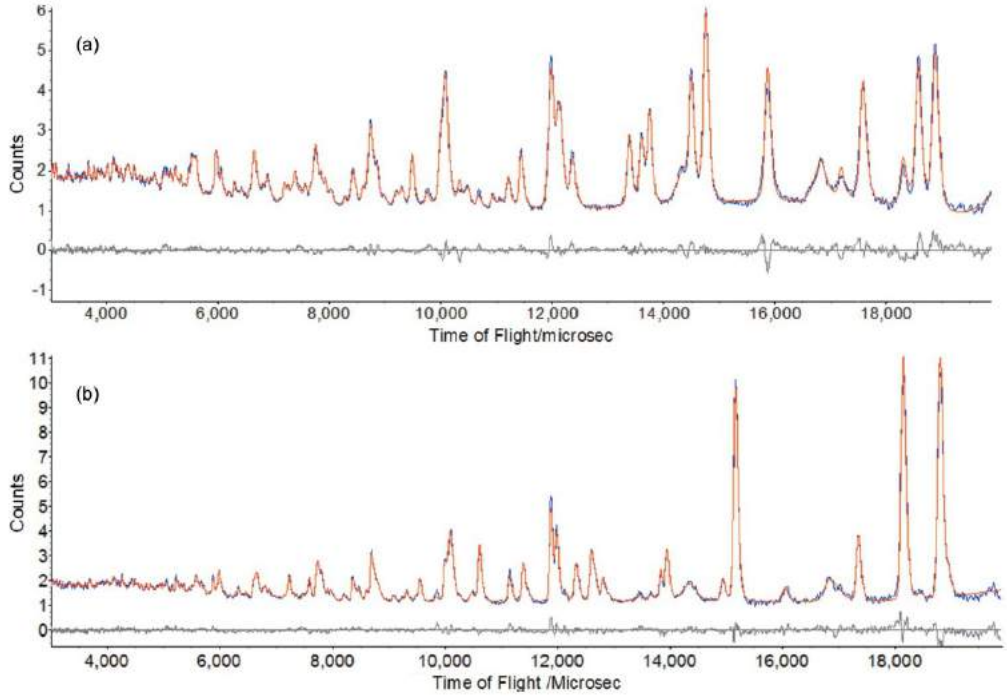

Figure 2
(*a*) Rietveld fit of the neutron powder diffraction pattern of ζ-glycine at 100 K (blue = observed, red = calculated). In addition to the peak ζ-glycine, the pattern also shows the presence of residual ε- and a trace of γ-glycine. Other peaks arise from the sample environment, namely tl pressure marker and the Al_2O_3 and ZrO_2 components of the anvils of the pressure cell. (*b*) Rietveld fit of the neutron powder diffraction patt β-glycine (contaminated with ζ- and a trace of γ-glycine) at 290 K. A 1 Å *d* spacing approximates to 4837 μs in time-of-flight.

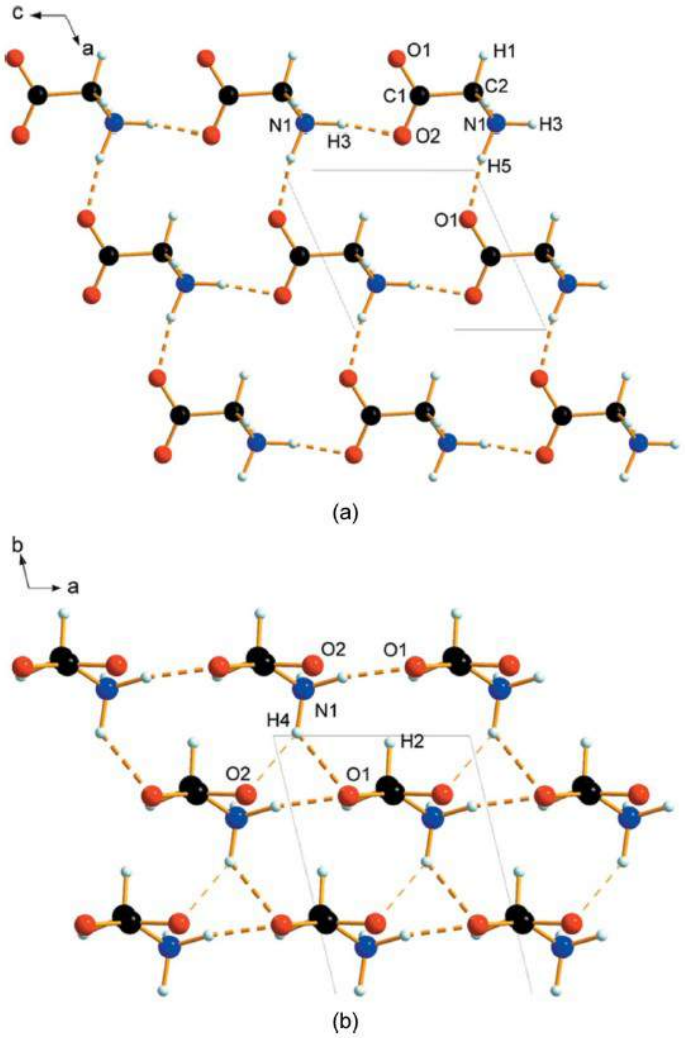

Figure 3
Intermolecular interactions in ζ-glycine. (*a*) Layers formed in the *ac* plane, viewed along **b**. (*b*) Stacking of the layers, viewed along **c**.

E Kucukbenli, CH Pham, SdG,
C Bull, G Flowitt-Hill, HY Playford, M Tucker, S Parsons
Int Union Crist J **4**, 569–574 (2017)

Credits

- Theory and Calculations

  Emine Kucukbenli, Cong Huy Pham

- Experiments

  C Bull, G Flowitt-Hill, HY Playford, M Tucker, S Parsons

- Networking

  Qiang Zhu

Controlling morphology of Au_{20} clusters by substrate doping

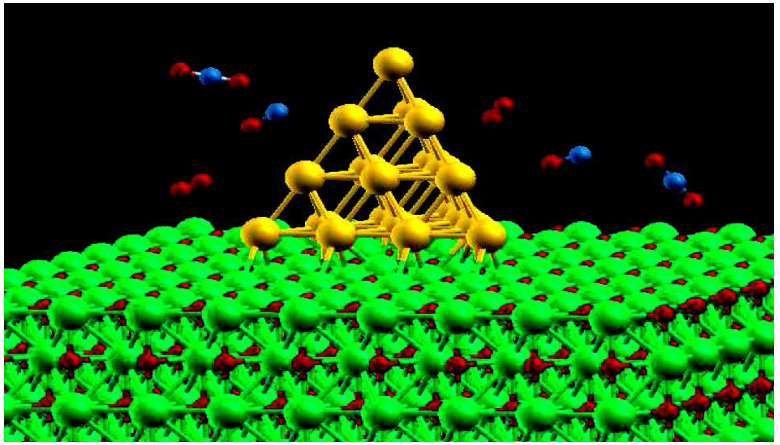

^{27}Al NMR shifts of Alumina and its precursors

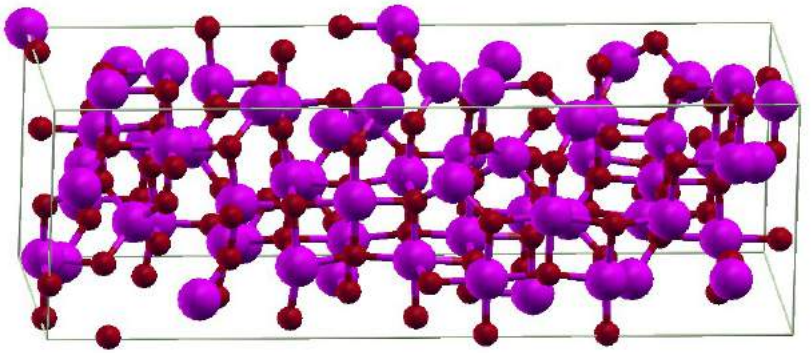

ζ-Glycine: Insight into the mechanism of a polymorphic phase transition

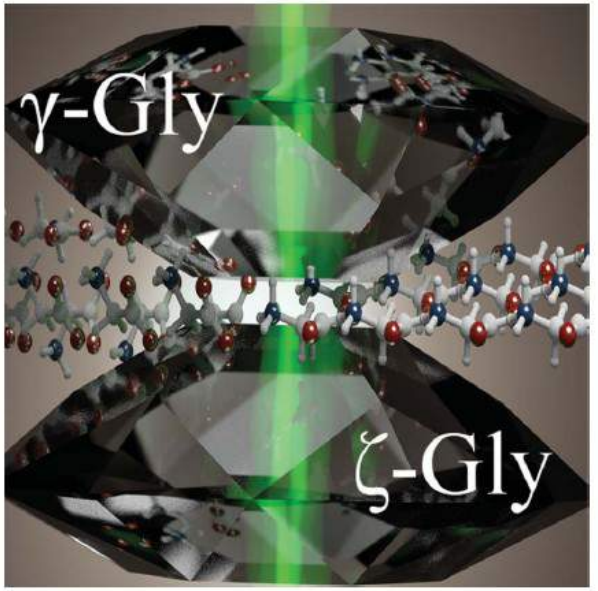

Complete ^{13}C Chemical Shift Assignment for Cholesterol Crystal

Thank you for your attention